Modeling Deep Infiltration from Irrigated Agriculture to Support Regional Water Management

A Thesis
Presented in Partial Fulfillment of the Requirements for the
Degree of Master of Science
with a
Major in Water Resources Engineering & Science
in the
College of Graduate Studies
University of Idaho
by

Bailey L. Olson

Approved by:
Major Professor: Jason Kelley, Ph.D.
Committee Members: Jerry Fairley, Ph.D.; Xiaoxue Du, Ph.D.
Department Administrator: Timothy Link, Ph.D.

December 2021

Abstract

Throughout the western United States, water managers are facing pressure to account for limited water resources among competing uses. Groundwater is one example of a limited resource that is continually being depleted, especially for areas that use groundwater for irrigated agriculture. In certain hydrologic systems, irrigated agriculture can contribute substantially to aquifer recharge through surface water infiltration, and thus is a significant water balance term for regional groundwater models. This thesis developed a bucket model to estimate deep infiltration by modeling soil water content and root water extraction. The model was calibrated with in-situ soil data from an irrigated alfalfa field and tested for model performance over two subsequent years of field data. The model was applied to a regional scale using test scenarios that account for differences in climate, management, and environmental factors. We show that for sprinkler irrigation methods with improved application efficiency, applied irrigation can contribute between 10-40 percent of deep infiltration losses under dry climate scenarios. While losses may occur at the field scale, these model results describe gains in aquifer recharge at the regional scale. Thus, the model provides an applied tool for more explicit estimates of near-surface boundary conditions for use in regional water management.

Acknowledgements

I want to offer much thanks to Dr. Jason Kelley, firstly for making himself available regardless of where we were physically located these past couple years. Dr. Kelley exceeded my expectations of what a graduate advisor should be, and took advantage of every teaching opportunity and offered encouragement to take on challenges I felt I wasn't ready for. He provided both academic and practical support during my time at UI, of which I am truly grateful for.

I'd also like to acknowledge my former colleagues at the Idaho Department of Water Resources, for making themselves available during my program for questions and great discussions on the agency's role in water management. I owe them credit for the opportunities I was given before graduate school, and recognize its key role in motivating the research presented in this thesis.

Dedication

I dedicate this thesis to my parents, Jared and Rebecca Olson. They have always encouraged me to push myself academically, and built my confidence in learning starting with piano lessons at 6 years old. They persuaded me to switch high schools, a decision I feel greatly altered the choices I would make down the road. I also want to thank my uncle, Daren, for his enthusiasm and help in applying for graduate school and fun discussions about all things water.

Table of Contents

List of Tables

List of Figures

List of Equations

Chapter 1: Literature Review

Introduction

The reliance on irrigated agriculture has created both thriving communities and uncertainties due to increased water demand and water shortages. For semi-arid regions in the western United States, irrigation is the difference between barren landscapes and productive farmland. Predominantly agricultural areas have experienced urban growth, which puts stress on total water availability as uses are divided between irrigation, municipal, domestic, and industrial. Climate change has also altered the availability of water. Mediterranean climates are forecasted to show earlier snowmelts with lower summer flows from increasing global temperatures (Vano et al., 2010). Agriculture in these regions require the right amount of water at the right time. The sustainability of irrigated agriculture relies on adaptive strategies to these current pressures.

Water resource accounting provides critical information on water supply and demand trends. A physically based approach to water accounting uses a water balance, which estimates inflows, outflows, and changes in storage within a hydrologic system. For some regional water balances, agricultural water use is a significant component. Approximately 72 percent of total global water extractions are used for irrigation (Cai and Rosegrant, 2009). A large portion of water extracted for irrigation is not returned to the system. Water that is not returned to the system is known as a "consumptive use". In the agricultural field, consumptive use of water refers to water that is directly used in the process of crop growth, or evapotranspiration (ET).

A body of research within the water resource field focuses on measuring ET from irrigated agriculture. Evaluating ET is useful for both farm managers, regional water managers, and researchers in efforts to promote agricultural sustainability. ET measurements help evaluate the productivity and efficiency of irrigation. In terms of regional water management, monitoring and forecasting water supply requires an understanding of the crop water use (ET). Evapotranspiration is increasingly relevant in the context of climate change scenarios, where ET has been shown to increase for southeastern Idaho by as much as 10% in the next 30 years (Huntington et al., 2015). Water policy is also concerned with crop water use, as groundwater aquifers are being "mined" at a rate that exceeds natural recharge. Recent litigation for the State of Idaho has sought to reduce aquifer withdrawals by 240,000

acre-ft-year (Miller et al., 2019). With agriculture being the largest consumer of freshwater supplies, providing science-supported ET estimates supports effective management and policy decisions.

ET Methods and Uncertainty

Evapotranspiration (ET) describes the combined processes of evaporation from the soil and transpiration from plant growth. These processes are combined as there is no easy way to distinguish them from each other. It should be noted that the evaporative component of ET only applies to water that leaves through soil evaporation. Evaporation is driven by weather related variables, including solar radiation temperature, humidity, and wind. Transpiration within agricultural systems is influenced by crop type and phenology, stressors like water shortage and disease, soil type, and farm management. Related terms used to describe ET include the crop water use, crop water requirement or demand, and consumptive use. Methods used to quantify ET must account for both weather and plant variables, and range in accuracy and complexity.

Methodology for estimating ET has grown significantly over the past century to include both ground-based and remote sensing approaches. In brief, ground-based approaches include simplified methods that estimate ET as the residual term of a water balance. These are common in large-scale hydrologic modeling. A popular on-farm approach is the pan evaporation method. This focuses on the evaporative "potential" of the surface from weather-driven variables and provides upper limit of ET a crop surface actually loses. Estimation of "actual ET" (hereafter ET_a) is the focus of this literature review, which usually involves more complex and costly methods like lysimeters, energy balance and mass transfer methods. More specifically, this review looks at modeling approaches that have developed over the past couple decades. These methods use remote sensing (RS) data to estimate actual ET from a surface energy balance. The following section first describes the theoretical background of estimating ET using surface energy balances. Second, an overview of a predominantly used RS model within Idaho water agencies, METRIC, is reviewed. Last, remote sensing ET models will be reviewed for their current use as both on-farm and basin-scale water management tools.

Mass and Energy Transfer Theory

Fundamental principles behind estimating ET are the law of mass and energy conservation. Evaporation, or latent heat flux, was described by Ira Bowen in his equation known as the Bowen Ratio (Bowen, 1926). This ratio describes the amount of heat transferred as sensible or latent heat and relies on surface gradient measurements of vapor pressure and air temperature. These methods were first developed over a surface of open water. Bowen's approach is still used today as the Bowen Ratio Energy Balance method (BREB). Uncertainties from this method are usually due to very low soil moisture (e.g., deserts) or where the area of study is non-uniform in fetch (Allen et al., 2011).

In 1948, Penman combined Bowen's energy balance with a mass balance method to account for water vapor removal above an evaporating surface. In effect, he was able to divide evaporation into two terms: first, the ability of the air to absorb water, and second, the amount of available energy to evaporate water from the surface. In the 1960s, John Monteith appended the work from Penman to account for influences of aerodynamic and surface resistances from a crop canopy (Farahani et al., 2007). Together, the Penman-Monteith (PM) method has become widely used since its standardization in 1990 by the Food and Agriculture Organization (FAO).

Reference ET and Limitations

FAO used the PM method to develop a standardized equation for calculating reference ET (hereafter ET_r). ET_r is defined for this equation as "a hypothetical grass reference crop with an assumed crop height of 0.12m, a fixed surface resistance of 70 s m-1 and an albedo of 0.23" (Allen et al., 1998). Subsequently, the American Society of Civil Engineers (ASCE) developed two reference crop ET equations (short grass and tall grass, or alfalfa) that were useable for daily or shorter time periods (ASCE-EWRI, 2005). The FAO and ASCE standardized methods were solutions to many documentation issues with ET research that existed up to that point and are still observed (Allen et al., 2011). Additionally, these institutions provided guidelines for analyzing the integrity of weather data before use in the reference ET equations.

Reference ET methods have been widely employed over the past half century. The development of the two-step method of estimating reference crop ET (ET_c) has aided the

applicability of ET estimation in the agricultural field (Allen et al., 1998). This method uses ET_r with a crop coefficient (Kc), which is the ratio of actual ET to the reference ET (as shown below).

Two-step method: $$ET_c = ET_r \times Kc$$

Crop coefficient: $$Kc = \frac{ET_a}{ET_r}$$

The Kc allows for adjusting the reference ET based on the crop's development stage. A more sophisticated approach separates Kc into soil and transpiration components to improve the accuracy of the Kc-ET_r method (Allen et al., 2005).

There remain inherent limitations to using the standardized reference ET equations. ET_r is based on ET rates from two generic crop types (short and tall) that are grown with uniform crop height under well-watered conditions. Applying crop coefficients does help account for certain variability in ET with crop type and growth stage, but actual ET could vary from the reference ET due to a variety of stress factors. Water stress is a factor that can cause reference ET to deviate from reference conditions. FAO accounts for this by using a water stress coefficient (Ks), which is based on a first-order function of soil water content. Other environmental stress factors, such as soil salinity, pests and disease, or soil fertility are accounted for a few crops by shortening the length of the mid-season crop coefficient (Allen et al., 1998). ET_r methods likely do not account for the variability of environmental factors that can affect rate of ET in both time and space. For instance, Allen describes influences of nearby surface types on reference ET estimates (2006). ET_r relies on representative weather data. It was found that dry or wet conditions upwind of the weather station can influence measured temperature and humidity that is used to compute ET_r for the measured reference surface (Allen, 2006).

Remote Sensing ET Models

Limitations of reference ET methods can be overcome in remote sensing models. In general, ET models require inputs of short and long-wave thermal imagery, provided by satellites with high spatial resolution. ET is calculated as the residual of a surface energy

balance. An energy balance approach captures the variability of surface conditions, including variability from crop type, stress factors like salinity, frost, and water shortages (Allen et al., 2011). Estimating ET through RS methods helps define an upper limit of ET based on the law of conservation of energy. ET rates that exceed the amount of net radiation at the surface can be flagged for data integrity. Ultimately, ET is calculated by estimating the transfer of sensible heat flux as follows:

$$ET = R_n - G - H$$

Where R_n is net radiation, G is sensible heat to the ground, and H is heat convected to the air above the surface. The difference in these terms represents the amount of latent energy used for ET.

METRIC

METRIC, or Mapping EvapoTranspiration at high Resolution with Internalized Calibration, is one example of a model that calculates ET as the residual of surface energy balance. This model has been used extensively in Idaho for water resource management (Allen et al., 2005), with applications in other regions of the world for irrigation scheduling (Santos et al., 2012). The model is used by Idaho Department of Water Resources (IDWR) in water rights accounting, groundwater pumping and recharge rate estimates, irrigation consumption, as well as computing water balances for basin scale hydrology (Bastiaanssen et al., 2005). METRIC uses thermal imagery from Landsat and a calibration procedure to set high and low ET rates for certain pixels. The high and low ET pixels are used to scale all pixels for the Landsat image to calculate ET_a in space. This calibration procedure uses ground-based reference ET at locations near the pixels of interest, which helps account for previous biases in remote sensing energy balances (Allen et al., 2007). Since the Landsat image only captures one instance of ET_a in time, the ET_a images or "maps" are interpolated over time for the entire year.

METRIC is an extension of the Surface Energy Balance for Land, SEBAL, which fundamentally shares similar methodology with METRIC. A unique approach by SEBAL and METRIC in calculating the near surface energy balance is their estimate of surface

temperature. The models use an air temperature gradient, dT, to describe a "blending zone" and eliminate the need for absolute surface temperature calibrations (Allen et al., 2007; 2011). A nuance in methods between METRIC and SEBAL relates to the evaporative fraction (EF), which is the ratio of ET to net radiation. In SEBAL, the EF is thought to remain constant throughout the day, especially in landscapes experiencing little change in soil moisture and wind (Bastiaanssen et al., 2005). Even though ET has a theoretical "ceiling" based on incoming net radiation, it has been shown that advective forces from upwind dry landscapes can cause ET to exceed the daily R_n (Allen et al., 2011). To account for this, METRIC uses hourly, gridded weather data to calculate the alfalfa (or tall crop) reference ET (Allen et al., 2005). ET_r is used to calibrate the model by finding the ratio of instantaneous ET (Landsat image of actual ET) to reference ET, like the use of a crop coefficient. Within the model this is known as the ETrF. The advantage of using ETrF is that the reference ET can capture regional advection affects that happen on shorter time steps than a day (Allen et al., 2007). Disadvantages of the METRIC model's approach in using ETrF is for rainfed systems where advection is low (Allen et al., 2011).

Limitations

One limitation of using the METRIC model is the need for manual calibration by a trained user familiar with physics of the energy balance (Allen et al., 2011). This calibration involves selecting "hot" and "cold" pixels within every thematic mapper (TM) image. The hot pixel represents a location in the image experiencing 0-10% ET_r (Morton et al., 2013). The cold pixel is the second calibration "anchor point" that represents maximum ET for all net radiation. Some of the drawbacks of the METRIC model requiring trained users has been solved in the automated calibration method (Allen et al., 2013). Since these "hot" and "cold" anchor points are the pixels at which the entire image is calibrated and have the potential to change for each user and each data change, automating the process has potential to increase accuracy between model runs. Morton et al. (2013) evaluated this automated method and found high ET pixels showed less uncertainty due latent energy being the remainder of net radiation and the ground heat flux. Low ET conditions showed more uncertainty since ET is calculated from large net radiation and sensible heat values.

Some fundamental limitations with using RS ET models deal with the resolution of

spatial and temporal data used to calculate the energy balance. Satellites will collect coarser spatial resolution with more frequent satellite overpass (e.g., higher temporal resolution) (Gowda et al., 2015). For Landsat images used in the METRIC model, the spatial resolution is 30 m with a fly over occurrence of 16 days. 30 m resolution is classified as high spatial resolution for satellite data, which is required for analyses at the field-scale. Larger pixel size can result in neighboring, non-field conditions adding uncertainty to water demand at the location of the field. In arid or semi-arid regions, farm-desert landscapes are predominant and is where this issue can arise (Gowda et al., 2015). Temporal resolution of RS ET models is too coarse for irrigation scheduling or soil water budgets that need to be made generally within the week, but other applications for these models for irrigation exist. For example, METRIC and SEBAL have been used within an irrigation scheduling tool to measure water requirements for cotton (Morari et al., 2020).

Applications in Water Management

For irrigation scheduling and water resource management at the field scale, both high spatial and temporal resolution of ET estimates are needed. Often with satellite data, there is a trade-off between spectral and spatial resolution. A few techniques have been used to enhance satellite imagery for agricultural water management, including downscaling and image fusion. In the downscaling methods, statistical tools are used to sharpen the thermal information on longwave bands. For instance, Tasumi et al. (2006) showed a linear relationship between surface temperature and the normalized difference vegetation index (NDVI), which serves as a useful method for semi-arid areas showing a stark contrast between vegetation and dry ground. In the image fusion method, multiple images from either the same or different sensors are combined to achieve higher spatial resolution. In many cases, image fusion will use multispectral and panchromatic images together to preserve the spectral and spatial resolution contributed by each, respectively (Ha et al., 2013).

The tradeoff in spectral and spatial resolution means water decisions must wait at least biweekly for high spatial resolution, which does not include the time need to process and publish this data. MODIS thermal data is a satellite product with 1 km resolution taken daily. The utility in using MODIS thermal data as an input to a surface energy balance ET

model is the temporal resolution increases from biweekly to daily. Larger errors in ET are found for upscaling methods, such as in Ershadi et al. (2013) which notes 15% reduction in ET due to decreased aerodynamic resistance at coarse resolution.

Though continued research is needed to evaluate possible effects of downscaling methods on ET uncertainty, there are several notable ways these techniques can be used. One example would be to use coarser ET data to match ground-based weather data. One extensive network of weather data is the California Irrigation Management Information System (CIMIS), which utilizes 145 automated weather stations to inform irrigators in efficient water management. The network provides continuous, hourly data used to calculate either grass or alfalfa reference ET, which can be multiplied by the crop coefficient for estimates of actual crop ET. Integrating ground-based measurements with satellite data can provide a clearer perspective on global weather patterns (Trenberth et al., 2014).

Another application provides general public with ET data in a web-based platform called OpenET. This app will largely provide monthly data at a 30 m resolution, estimated at a field-by-field scale for data going back to 2018. The data used within OpenET includes several existing ET models, including METRIC, SEBAL, ALEXI, SIMS, and others (*https://openetdata.org/intro/*, *Accessed October 2021*). This application takes an average of all ET models to yield one ensemble average, which reduces confusion with model accuracy and provide greater accessibility to all users. The development team is also conducting a wide-scale assessment of satellite data accuracy used in the platform by comparing data with eddy flux towers, groundwater pumping records, and basin-scale water balances.

In quantifying agricultural water use in the ESPA, the OpenET platform shows two major advantages. First, the platform has provided at least two years of recent data from several ET models, which allows the proposed research to use an ensemble average for all ET analyses. Second, the platform has incorporated spatially explicit information at the field scale, including the capability to integrate a water rights database and view cropping types for any given field. This has several merits in agricultural research, such as accounting for interannual variability between crop rotations and changes in irrigated acreage. The potential to look up Place of Use (POU) and the associated water rights will provide information about the water source and validate ET estimates through any existing pumping records.

The review of literature has shown ET estimations can vary in accuracy and

complexity, though RS ET models show the greatest potential to quantifying ET for basin-scale water management. RS models also account for spatial and temporal variability of ET missed in using standardized reference ET methods. The uncertainties of using RS models largely depend on the physical assumptions underlying the model's algorithms, as well as the spatial resolution of the satellite data used in the model. Continuing to validate satellite-based ET with ground-based measurements is likely needed to support ET research.

Non-Consumptive Water Use: Deep Infiltration

The previous sections of the literature review overview methods of estimating evapotranspiration, which can play a significant role in regional water balances. This is especially true for areas with irrigated agriculture, where irrigation accounts for about 90 percent of consumptive water uses globally (Siebert et al., 2010). Consumptive use in context of irrigation describes water lost to the atmosphere and cannot be recovered elsewhere in the hydrologic system. The remaining 10% of water not consumptively used from irrigation can contribute to surface runoff, wind loss, or deep infiltration. This latter term, deep infiltration (DI), will be used throughout this thesis to describe water that moves vertically past the effective rooting zone of a crop, and is thus unavailable for root water extraction that contributes to ET. Similar terms to DI presented in the literature include seepage or deep percolation.

Deep infiltration has relevance today as water managers face pressure to account for limited water resources among competing uses. Groundwater is one example of a limited resource continually being depleted, especially for areas using groundwater for irrigated agriculture. Irrigated agriculture has potential to contribute substantially to groundwater recharge, especially with irrigation methods such as flood or furrow irrigation. Within the past decade, more efficient irrigation methods such as overhead sprinkler systems reduce the amount of irrigation applied to the surface. Chapter 4 of this thesis provides an example for southern Idaho, where improved irrigation efficiencies have reduced recharge to the aquifer. Since irrigated agriculture accounts for the largest freshwater withdrawals globally, it is often the targeted water user in which water conservation can be improved. Governments have provided subsidies to promote water savings by adoption of irrigation efficiency technologies, but these have often failed to meet the end objectives (Grafton et al., 2018).

In order to evaluate the impact irrigated agriculture has on water resources, robust water accounting efforts are needed. Often, water managers rely on the conservation of mass and water balance methods to keep track of inflows and outflows to a hydrologic system. Deep infiltration is one part of field and regional water balances that is difficult to measure. Established methods often estimate DI as the residual of surface water diversions less evapotranspiration. While spatially explicit measurements of ET improve DI estimations, the infiltration process is largely driven by soil mechanics. It is regarding these physically based processes that regional water accounting could use improved tools, even if they simply offer a first order approximation of DI. The following will review general methods of estimating infiltration rates using physically and empirically based equations, and then describe a few modeling approaches to estimating deep infiltration.

Infiltration Methods

The process of infiltration is difficult to quantify, largely due to the heterogeneity of soil systems and the complexity of soil and water interactions in time and space. Current methods of quantifying infiltration can use physically-based equations, empirical equations, and in situ measurements. The Darcy equation is a well-known physically based method that describes water flow in a one-dimensional, homogenous soil profile. It can be written as follows:

$$q = -K\frac{\partial \emptyset}{\partial z}$$

Where q is the velocity of a volume of water moving through the soil in the z direction per unit of area per unit time, K is the hydraulic conductivity, and $\frac{\partial \emptyset}{\partial z}$ is the hydraulic gradient (Ward et al., 2016). The hydraulic conductivity K is a function of soil water content and pressure head, where the negative sign describes that flow will occur from high pressure to low pressure. Subsequently, Darcy's equation was adapted to describe unsaturated flow with the Richard's equation. The Richard's equation uses Darcy's equation with an included term for soil water diffusivity. Challenges to using the Richard's equation are due to the non-linear relationship between soil water content, hydraulic conductivity, and pressure head

(Ward et al., 2016).

Empirical methods of estimating infiltration include the Horton equation and Green and Ampt equation. Horton's method relies on only three parameters but must be calibrated with field data. Additionally, the parameters have no physical basis. Green and Ampt coupled the physics of soil water movement by Darcy with empirical parameters that are physically significant. In brief, Green and Ampt estimate infiltration by accounting for the wetting front, which captures process that wick moisture upwards from drier to wetter soils. While the equation is developed for homogenous soil conditions with uniform initial soil water content, calibrating the equation with in situ data could yield accurate estimates for heterogenous soils. Ward et al. (2016) provided their own literature review on infiltration methods, and coupled with the author's research experience, conclude "there is no single equation that works well for all situations". Kale and Sahoo (2011) also emphasized infiltration models need to account for layered soils with varying initial soil water contents. Additionally, it is likely "piston" type of flow described by Richard's and Green and Ampt equations are not the main mechanism driving infiltration in agricultural soils, since these soils are ubiquitous for macropore flow (Ward et al., 2016).

Modeling Deep Infiltration

The research objective for this thesis is to develop a model that can be used to quantify infiltration occuring below the root zone of a crop (i.e., deep infiltration). This will be done by coupling a water balance with process-based components to model water movement and root water extraction from irrigated crops. Components of soil water balances are difficult to measure directly and rely on estimations. Regional water management currently use water balance methods, which are simplified calculations used to estimate DI as the residual of surface water diversions and ET. Mechanistic or empirical equations described in the previous section can be used to capture the dominant processes that describe soil water movement. These equations are used within complex models, such as the Deep Percolation Model by United States Geology Survey (USGS), MODFLOW, and HYDRUS-1D (Šimůnek, 2015) require a certain amount of input data, user knowledge, and processing power to run. These groundwater flow models, in addition to crop growth models, like CropSyst (Stockle and Nelson, 1996) and soil erosion models, such as SWAT

(Arnold et al., 2012), estimate DI as a concomitant to main output variables. The Deep Infiltration Model presented in this thesis fills a gap between simplified water balance methods and modelling tools that may not be easily applied for regional water management.

The development of the Deep Infiltration Model for this thesis was guided by research done by Liu et al. (2006), where water balance models were coupled with empirical methods to estimate deep infiltration from the root zone. The solution proposed by Ogata and Richards (1957) was used to estimate drainage that occurs within a day, and is shown as follows:

$$W = at^b$$

Where W is the soil water storage in the root zone, and a and b are empirically derived soil parameters describing soil drainage over one day. This equation was modified to compute soil drainage from day $i+1$, which is shown in Table 2.1 of Chapter 2. Deep infiltration is computed as the difference of soil water storage on day i and day $i+1$ (Table 2.1).

Soil parameters a and b were determined for silt-loam soils in North China. Liu et al. (2006) notes that these parameters can be estimated for other soils based on the following guidelines:

$$a\text{: soil water storage value between } W_{FC} \text{ and } W_{SAT}$$
$$b < -0.0173 \text{ for fast draining soils and}$$
$$b > -0.0173 \text{ for slow draining soils}$$

Where W_{FC} and W_{SAT} are soil water storage at field capacity and soil water storage at saturation, respectively. “Field capacity” is soil water storage after 1-2 days drainage, and is often described as the soil suction pressure of -33 kPa. These guidelines were used as a baseline estimate for soil parameters used to calibrate the Deep Infiltration Model and test model performance. The method presented by Liu et al. (2006) was used because of its incorporation of a water balance as well as its simple parametric approach to calculating soil drainage over a daily timestep.

Chapter 2: Deep Infiltration Model

Introduction

Water resources in the Western United States are facing increased shortages, hastening policy and planning decisions to ensure future demand meets supply. Some adaptive decisions to water shortage focus on the supply side of the issue, such as desalination of ocean water in coastal communities. This is a costly solution compared to traditional sources of water, and only meets a small fraction of total water demand. When augmentation of supply is not practical, which is often the case, the demand side of water resources is evaluated. In California, frequent droughts have been attributed to climate change and have led to "blanket curtailments", which are state mandates preventing many water right holders from withdrawing their allocation. This imposes hardships on farmers in regions who rely on irrigation to support crop production. Some suggest such drastic measures would be unnecessary if water resource agencies better accounted for actual water usage (Grantham and Viers, 2014). Others suggest implementing water markets improves the efficiency of water resource management in the face of climate change (Adler, 2009). Owen (2014) warns both approaches are "practically and legally intertwined," and require an understanding of the "ripple effects" of management decisions within hydrologic systems.

The irrigation sector plays a substantial part in hydrologic systems in the west and worldwide. Global statistics show irrigated agriculture constitutes about 72 percent of total water extracted from freshwater and groundwater supply (Cai and Rosegrant, 2009). Water used by irrigation is unique from other sectors, since a large portion of applied water is used consumptively and not returned to the water system. Consumptive use in agriculture describes evaporation and crop transpiration, which is collectively called evapotranspiration (ET). Grafton et al. estimates consumptive use from agriculture between 40-85 percent of total application for varying irrigation methods (2018). The remaining non-consumptive fraction of total applied water returns to the water system, either through surface runoff or deep infiltration.

Consumptive and non-consumptive use are terms that support water policy goals by explicitly defining how water is used and its availability for other water uses in a larger system. These metrics aid in water accounting at various scales and provide tools to promote the sustainability of irrigated agriculture. Water accounting at the farm-scale is useful to

producers. With increased pressure on water supply, many producers are shifting towards maximizing the productivity of water. One way to accomplish this is by scheduling irrigation based on the crop water demand (ET). Irrigation is meant to supplement the amount of soil water depleted through root extraction. Irrigators who understand the root zone depth and soil holding capacity of their field are able to use water efficiency in terms of applying only the amount lost to crop ET. Excess irrigation overfills the soil reservoir and causes deep infiltration (DI) below the zone accessible to roots. Excess irrigation can also lead to unfavorable outcomes like nutrient and chemical leaching, waterlogging, or salination (Howell, 2001). Additionally, overall energy use and pumping costs from irrigation can decrease significantly with careful management (Ross and Hardy, 1997).

Water accounting of irrigated agriculture is useful in basin-scale water management. The non-consumptive portions of irrigation, namely runoff and deep infiltration, return to the hydrologic system for other uses. Many systems exhibit a certain degree of hydrologic connectivity, a term used here to describe the linkage of surface and groundwater sources. A notable example from southern Idaho found inefficient irrigation methods create substantial amounts of deep infiltration, thereby recharging the underlying aquifer and creating greater spring flows down gradient. The on-farm inefficiencies from DI cause water to be made more accessible for other uses. These uses include heighted aquifer levels for groundwater pumpers, constant water temperatures for fisheries, and hydropower production from spring flows (Willardson et al., 1994). Runoff also increases in-stream flows, though this tends to have negative impacts to surface water quality.

There is clear utility in water resource accounting for irrigated agriculture, but methods to do so are often complex. Accounting for deep infiltration is specifically challenging, as it is a subsurface process that can occur over widespread areas at varying time scales. Direct measurements are limited to lysimeter experiments (Bethune et al., 2007; Hatiye et al., 2016). Lysimeter equipment is not feasible for basin-scale water accounting, smaller budgets, or those unfamiliar with the equipment. Modeling approaches for estimating DI exist, though require certain input data and user knowledge. The United States Geological Survey (USGS) has published the Deep Percolation Model, which estimates groundwater recharge for large areas over varying landscape and land use conditions (Vaccaro, 2007). This model is part of the modular system USGS employs to simulate groundwater flow in aquifers with

MODFLOW. A solute transport model, HYDRUS-1D, has been used to model groundwater recharge for near-surface water balances (Šimůnek, 2015). A regionally based model, ESPAM, focuses on recharge and spring flow discharge for Idaho's principal aquifer (Sukow, 2021). Other models estimate DI as a concomitant to main objective outputs. These include the crop growth simulation model, CropSyst (Stockle and Nelson, 1996), soil erosion and groundwater pollution model, SWAT (Arnold et al., 2012), and climate models, EPIC and APEX (Gassman et al., 2004). These are numerical models, and their use are restricted to trained personnel and are not suitable for most farmers attempting to manage their water use.

Study Objectives

With varying approaches to deep infiltration estimates, the main objective for this study was to provide an applied tool that estimates DI by simulating soil moisture for irrigated crops. This was accomplished using a soil water balance model with accompanying equations used to estimate soil water drainage. A daily soil water balance accounts for major fluxes of water within the root zone of an irrigated crop. The model was calibrated with actual ET and soil moisture data observed for an irrigated crop and tested with field data collected for other years. Model testing using subsequent years of soil data help build confidence in the model's ability to simulate soil moisture data, considering interannual variation in weather and soil moisture.

This model shares similarities with an irrigation scheduling tool built by Washington State University (Peters et al., 2019). The "Irrigation Scheduler" is a weather-based tool with a soil water balance approach of modeling total available water (TAW). The TAW is a term used in data-based irrigation scheduling describing the percentage of volumetric water content available for root water extraction. The model accounts for crop and soil type, the crop water requirement (ET), as well as water stress and deep infiltration losses. Water stress and DI are also a function of the root zone water content. The current study extended on the Irrigation Scheduler approach by modeling stress as a function of soil water potential (i.e., capillary suction) rather than water availability. In this way, water stress is estimated as an intensive variable based on the energy state of soil water.

The main motivation for this model was to evaluate the impact of irrigation technol-

ogy on basin-scale water balances. With increased water shortages and competition for irrigation, understanding the impact of new adoptive strategies like irrigation technology will be important for future policy and management decisions. This tool can be applied at scales in which these decisions are made and provide an approximate range of values for DI. Deep infiltration estimates are important to both producers and water managers. For a producer, they represent water and energy losses. For water management, DI is one source of aquifer recharge for groundwater dependent regions. Lastly, hydrologic assessment of irrigated agriculture provides another facet of science-based factfinding to inform climate change initiatives of today.

Model Design

The following describes basic design components and assumptions for the Deep Infiltration Model. Background information pertinent to estimating soil water content parameters are also described.

Model Overview

The DI model is a one-dimensional, soil water balance model that simulates daily soil water content (SWC) for irrigated crops for the length of the irrigated season. The model focuses on an applied approach with input parameters accessible to general farm managers, such as irrigation schedules, soil texture and depth, and weather data used to describe crop water use. Two soil drainage parameters (Table 2.1, Equation 2.1) are the adjusted variables used to calibrate the model. The dependent variable, deep infiltration, is derived using a daily soil water balance. DI is defined in this study as soil water that percolates below the lowest vertical boundary of the root zone, the latter of which describes the model boundary. The model was calibrated using the first soil layer within the root zone. The first layer is set to the representative depth of soil sensor data used to force the model to observed conditions. Sublayer soil water contents were simulated without the use of calibration data.

Functions within the model are categorized either as process-based or time-series based (Table 2.1). Process-based calculations are focused on simulating natural phenomena of crop growth and root water extraction (RWE). The time-series calculations are time explicit and capture the major inputs and outputs of the system occurring at a daily time step.

Evapotranspiration represents a major output from irrigated agriculture and is represented in two ways within the model design. First, actual evapotranspiration (ET_a) was used as a forcing variable in modeling soil water content for the surface layer. Second, crop evapotranspiration (ET_c) was derived using methods found in Allen et al. (1998) for model simulations in Chapter 3.

This model does not account for the following processes that could factor into soil water movement within the root zone: surface runoff, surface run-on, capillary rise from shallow aquifer tables, temporary surface storage (ponding), preferential flow, or other flow influences like water and soil chemistry and air entrapment (Wang et al., 1998). Precipitation is also not considered as the model focused on semi-arid regions with few rainfall events. Lastly, this model was based on rooting depth and root mass distribution for alfalfa. Future development of this model could consider variation in RWE and DI for different crop types.

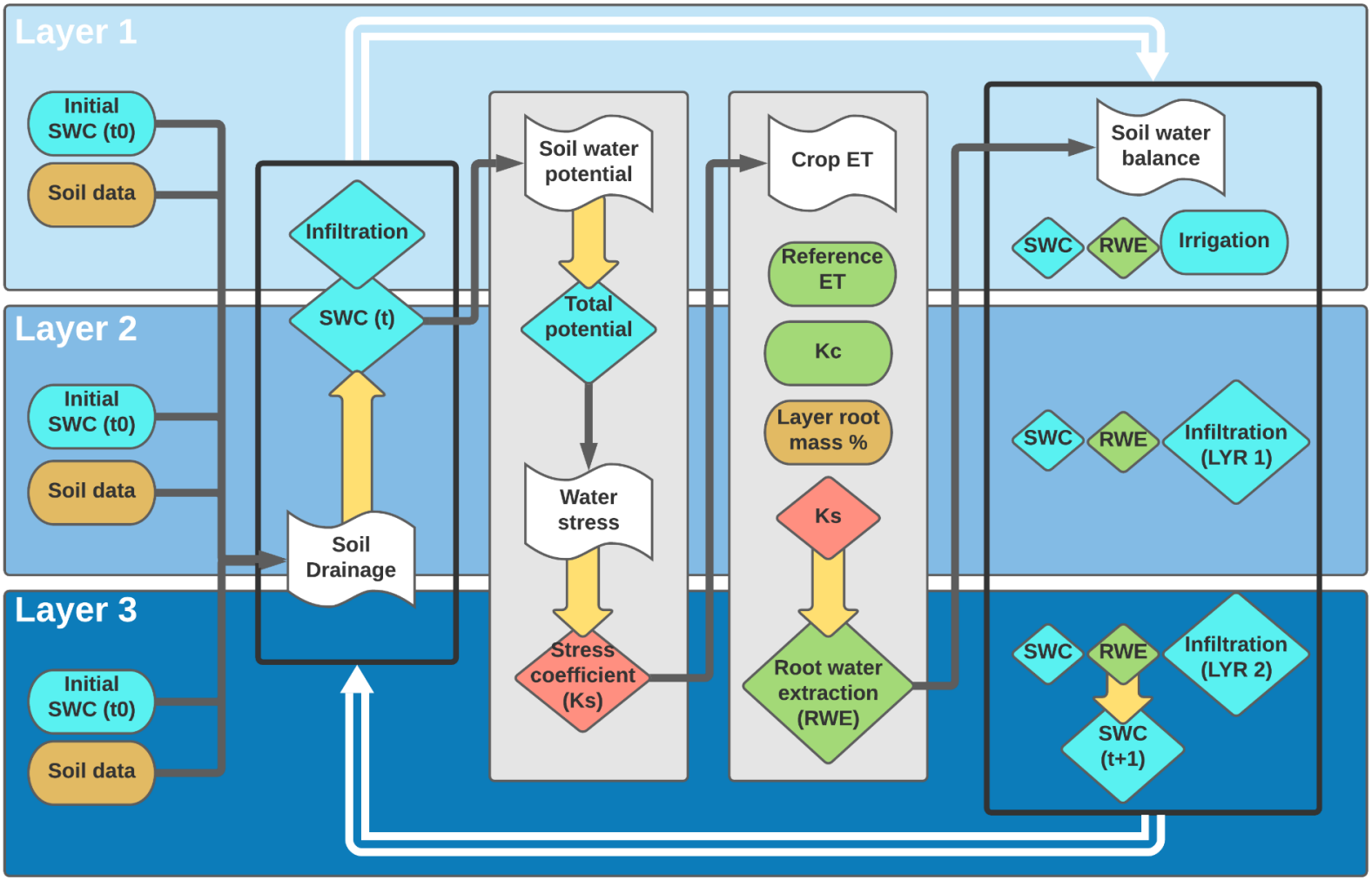

Figure 2.1 Schematic for the Deep Infiltration Model. Primary input parameters are shown on the far left as oblong shapes. Black arrows show the order of operations, where the white arrows indicate how the model operates iteratively. Computations are indicated as white tape, where yellow arrows mark the output from each function. Variables are shown as diamonds. Greyed boxes indicate what functions are performed collectively for all modeled layers, where "clear" boxes are functions calculate for each separate layer. Color coding of schematic parameters/variables are represented as follows: soil water (blue), soils data (brown), crop water requirement (green), and stress factors (red).

Table 2.1 Functions Used in the Deep Infiltration Model. The "DI" variable is denoted here to represent infiltration processes from all soil layers.

Function	Type	Description	Input/Description		Primary Equation(s)	Equation
Soil Drainage	Time Series	Decay function for soil water content on *i+1* (Liu et al., 2006; Wilcox, 1959). DI is calculated using *SWB* from equation 2.11.	*SWC* *a, b* SWB	Soil water content Drainage constants Soil water balance	$SWC_{(i+1),\ LYR(i)} = a\left[1+\left(\frac{SWB_{i,\ LYR1(i)}}{a}\right)^{\frac{1}{b}}\right]^{b}$ $DI_{(i+1),\ LYR(i)} = SWB_{(i),\ LYR(i)} - SWC_{(i+1),\ LYR(i)}$	2.1 2.2
Soil Water Potential	Process	Calculates total soil water potential, Ψ_T (Eq. 3). Matric potential (Eq. 5) is calculated using pedotransfer function by Saxton and Rawls (2006).	Ψ_g Ψ_m G H A *B*	Gravitational potential Matric potential Gravity constant (9.8 m s^{-2}) Vertical height [m] from soil surface Soil-moisture coefficients	$\Psi_T = \Psi_g + \Psi_m$ $\Psi_g = GH$ $\Psi_m = \mathrm{A}(SWC_{(i)})^{-B}$	2.3 2.4 2.5
Water Stress	Process	Piecewise stress functions relating soil water potential (Ψ) to a water stress factor, "Ks" (values 0-1). Not shown is when $\theta_{FC} \leq \Psi_T < \theta_{MAD}$, Ks = 1 or no water stress conditions, and when $\theta_{WP} \leq \Psi_T$, Ks = 0.	Ψ_{FC} Ψ_{MAD} Ψ_{WP} (*sat*$_{m,b}$, *unsat*$_{m,b}$, *unsat*$_{b1,b2}$) *d*1	Ψ at field capacity Ψ at management allowable depletion Ψ at wilting point Soil constants for linear and decay equations $0.40(\theta_{MAD} - \theta_{WP})$	$if\ 0 \leq \Psi_T < \theta_{FC}\ then$ $Ks = (sat_m)\,\Psi_T + sat_b$ $if\ \theta_{MAD} \leq \Psi_T < d1\ then$ $Ks = (unsat_m)\,\Psi_T + unsat_b$ $if\ d1 \leq \Psi_T < \theta_{WP}\ then$ $Ks = unsat_{b2}\,(\Psi_T)^{unsat_{b1}}$	2.6 2.7 2.8
Crop ET	Process	Determines the amount of root water extraction (RWE) based on the reference ET and crop coefficient (Allen et al., 1998).	ET_r Kc pct_x Ks	Reference ET Crop coefficient Weighted factor for root mass Stress coefficient	$RWE = ET_r\,Kc\,(pct_x)\,Ks$	2.9
Soil Water Balance	Time Series	Layer 1 receives irrigation (Eq. 2.10), where lower layers receive upper layer infiltration (Eq. 2.11).	IRR AE RWE DI	Irrigation Application efficiency Root water extraction Deep infiltration	$SWB_{(i+1),\ LYR(1)} = SWC_{(i),\ LYR(1)} - RWE_{(i)\,LYR(1)} + IRR_i$ $SWB_{(i+1),\ LYR(i)} = SWC_{(i),\ LYR(i)} - RWE_{(i)\,LYR(i)} + DI_{(i),\ LYR(i-1)}$	2.10 2.11

Table 2.2 Parameters for the Deep Infiltration Model.

Parameter	Unit	Description
IRR	mm	Daily irrigation schedule
ET_r	mm	Reference evapotranspiration (Allen et al., 1998)
Kc	-	Crop coefficient (Allen et al., 1998)
ET_a	mm	Actual evapotranspiration
sens_depth	mm	Representative sensor soil depth layer for model layer 1
num_lyrs tot_depth vert_h	mm	number of model layers (3) total root zone depth (120 cm) Vertical height of soil layer from surface (20, 70, 120 cm, for layers 1-3, respectively)
pct_max_min	fraction	Describes the slope used to define the pct_x factor (Eq. 2.9) (fixed value at [0.60, 0.50])
b, all layers	negative fraction	Constant for use in Eq. 2.1, describes the drainage rate
a, all layers	fraction	Constant for use in Eq. 2.1, approximated as SWC between SAT and FC (Liu et al., 2006)
$SWC_{(i)}$, all layers	mm	Initial soil water content
A, all layers B, all layers	-	Soil moisture coefficients (Eq. 2.5), estimated via pedotransfer functions (Saxton and Rawls, 2006)
θ_{SAT}, all layers θ_{33}, all layers θ_{1500}, all layers	volumetric water content (VWC) [%]	VWC at saturation VWC at 33 kPa VWC at 1500 kPa (Saxton and Rawls, 2006)
IRR_{eff}	fraction	Irrigation efficiency factor, otherwise known as the application efficiency (AE)

Model Functions

The following sections cover two model functions in further detail, namely "Water Stress" and "Crop ET" (see Table 2.1). These are processed based functions used to simulate crop growth and root water extraction (RWE). The "Crop ET" function was not used in the calibration or validation process of the model, as actual ET (ET_a) and observed SWC were used as forcing parameters to simulate layer 1 with observed soil conditions.

Water Stress

Water stress is accounted for in the Deep Infiltration Model using a piecewise continuous function relating total soil water potential to a dimensionless water stress coefficient (Ks). The model attributes a Ks value between 0-1 for each soil layer defined in the model. The main input to the Water Stress function is total soil water potential (Ψ_T) and soil water potentials at field capacity (FC), management allowable depletion (MAD) and wilting point (WP) for a given soil type. These latter terms are typically used for irrigation management to describe the water holding capacity of the crop's root zone. FC is defined as the soil water content when the soil suction or potential is between 10-33 kPa (Ward et al., 2016). The wilting point is the soil water potential at which the crop cannot extract water and is irreversibly wilted (~1500 kPa). Management allowable depletion is between FC and WP and is an estimation of soil water potential at which the plant experiences water stress. Irrigation is ideally kept between FC and MAD, since above FC the plant can experience saturated water stress.

For the Water Stress function, three linear equations and a decay curve are used to attribute Ks based on total soil water potential. A linear equation is used to describe saturated soil conditions, where the domain values are between 0 and soil water potential at FC (Ψ_{FC}). Between Ψ_{FC} and Ψ_{MAD} the stress coefficient is equal to 1. Below Ψ_{MAD} the Water Stress function estimates unsaturated soil moisture potential with a linear equation and decay curve. The point at which the linear equation ends is at the coordinates (*d1, d2*) as shown on Figure 2.2. Domain value for *d1* was arbitrarily assigned as equal to $0.40(\Psi_{WP} - \Psi_{MAD})$, where *d2* was set at Ks = 0.15. The decay curve constants are assigned so that Ks is approximately equal to 0 when the curve approaches Ψ_{WP}.

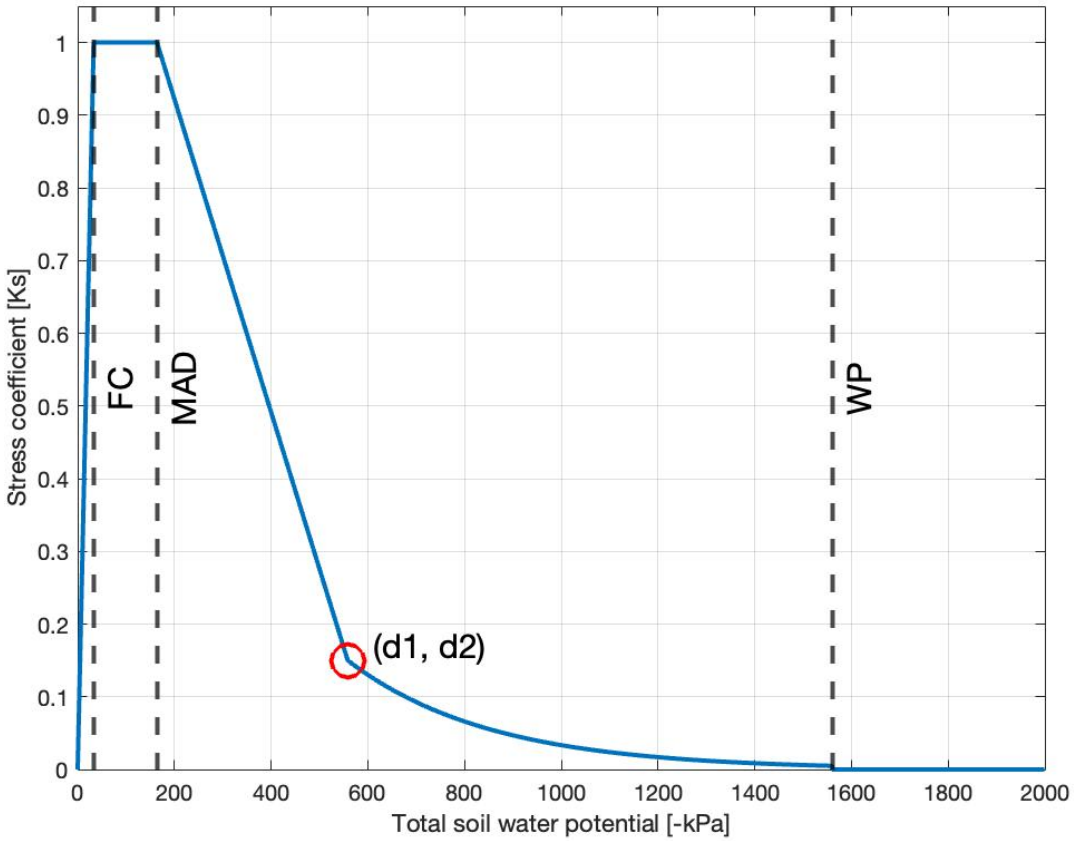

Figure 2.2 Water Stress Piecewise Function. Terms used for water management (i.e., FC, MAD, WP) are indicated as dashed lines. The coordinates (*d1, d2*) are shown to indicate the end of the unsaturated linear equation and the beginning of the decay curve. The input parameters used in this figure were based on soil types given for model calibration and validation data.

Crop ET

The Deep Infiltration Model uses the two-step method to calculate crop ET (ET_c) as a function of reference ET (ET_r) and a crop coefficient (Kc). This method is covered in the FAO-56 paper and is also known as the "crop coefficient approach" (Allen et al., 1998). ET_r is calculated using the FAO Penman-Monteith equation. More information on this method is covered in Chapter 1. The process of estimating Kc for alfalfa is described in Chapter 3. The DI model uses the daily ET_r, Kc, and Ks to calculate the amount of root water extraction (RWE) for each model layer (Table 2.1, Eq. 2.9). An additional parameter, "pct_x", is a non-dimensional weighted factor that scales the amount of RWE based on the soil layer depth and root mass. Since the model was calibrated and simulated for alfalfa crops only, the pct_x factor is based on alfalfa for three separate soil layers, totaling a maximum rooting depth of 120 cm.

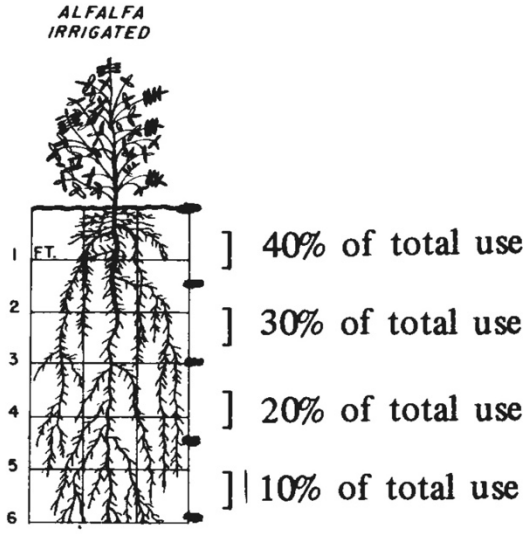

Figure 2.3 Irrigated Alfalfa Root Water Extraction Distribution. Figure credit: (Bauder, 1978).

The illustration in Figure 2.3 is one commonly cited distribution for the relative RWE for irrigated alfalfa. This distribution is both a function of root depth and root mass. Generally, greater root mass and root water extraction comes from the upper soil layers. This supports the theory plants conserve energy by shortening the distance required to move water up through the plant structure.

Since the model allows for the user to define the number of soil layers and layer width, a "pct_max_min" parameter is used scale RWE based on these inputs. The pct_max_min requires a maximum and minimum fractional value describing the percent RWE from the top and bottom of the root zone. For model calibration and simulation in Chapter 3, these were fix values of (0.60, 0.50). For a deeper rooting zone for alfalfa or related crops, the pct_max_min may be adjusted more closely to Figure 2.3 (i.e., 0.40 and 0.10). These fractional values are used to calculate a slope for a simplified linear function that calculates pct_x (i.e., RWE) as a function of soil layer depth.

Calibration and Performance

The following describes methods and materials used to calibrate the surface layer of the model with in-situ soil data collected at an alfalfa field in Harney Basin, Oregon.

Background on field data

Data used for model calibration and validation were collected at an irrigated alfalfa field about 30 miles (48 km) southeast of Burns, Oregon. The alfalfa field is located within the Harney Basin Watershed, which receives about 6 inches (15 cm) of annual rainfall (Figure 2.5). The basin is currently undergoing research by USGS and partners to characterize groundwater flow in the area and address gaps in understanding. The watershed is used extensively for agriculture with reliance on groundwater resources for irrigation. USGS research focuses on addressing uncertainties surrounding surface and groundwater interaction, and how this might impact water right holders in the area (*https://www.usgs.gov/centers/or-water/science/harney-basin-groundwater-study*, *Accessed Oct 2021*). The current study has implications for water management in this region though they are not specifically addressed.

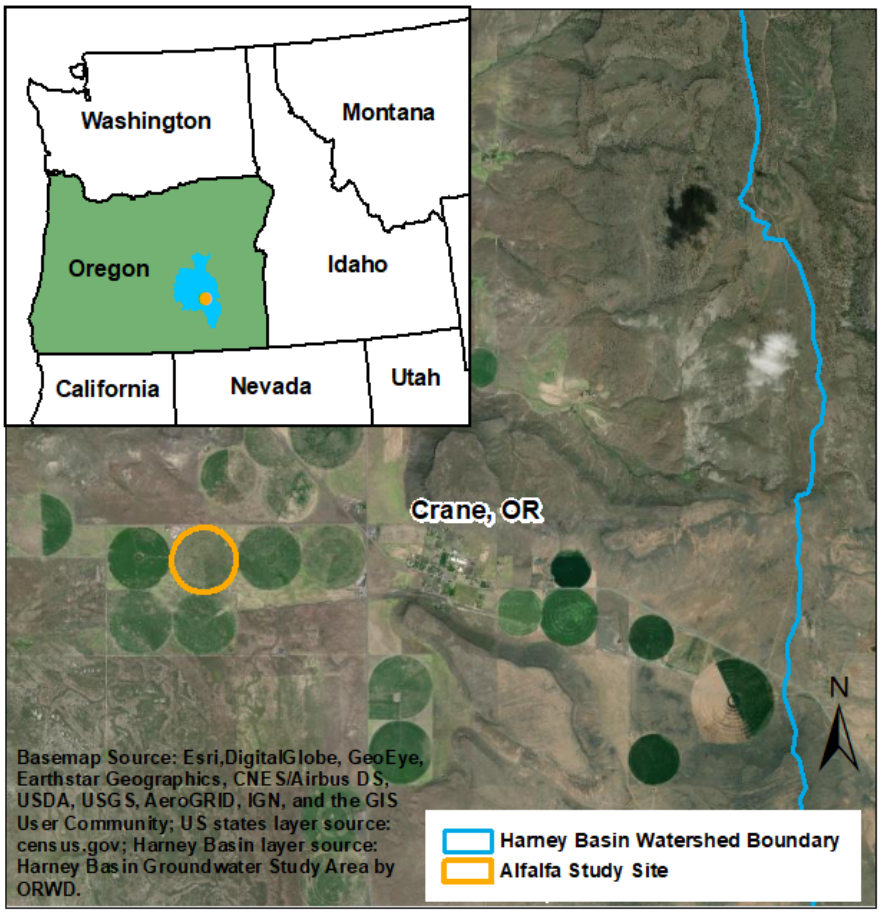

Figure 2.4 Harney Basin Alfalfa Field Site.

Historically, large rainfed lakes dominated the watershed. Soils found in the basin relate to old lake terraces and lake beds as well as alluvial deposits. The dominant soil type for the alfalfa site was determined using the Web Soil Survey by the Natural Resources Conservation Service (NRCS) (*https://websoilsurvey.sc.egov.usda.gov/App/HomePage.htm*, *Accessed June 2020*). Soils for the alfalfa field are under the "Poujade series", which are well-drained fine sandy loams. Soil texture properties for this series were used to define model parameters.

Input Data

The following describes input data used in model calibration and validation. Forcing parameters, which include observed SWC and ET_a collected at the field site, were used to constrain simulated behavior of soil water content in the root zone. These parameters aid in quality assurance by creating boundaries for model output that are realistic for observed conditions.

Soils Data

Soil water content (SWC) data measured at the alfalfa field were used to calibrate the first layer of the DI model. Data were collected from two CS616 Water Content Reflectometers (Campbell Scientific Inc., Logan, UT, USA) installed about 2.5 cm below the soil surface. Probe rods oriented vertically indicate SWC for the upper 30 cm of soil (Campbell Scientific Inc., 2020).

Figure 2.5 Soil Water Content Sensor Installation at Harney Basin Alfalfa Field.
Photo credit: (R. Jasoni, *Retrieved June 2020).*

Raw SWC data were corrected for apparent sensor drift and values unrealistic for the given soil type. For example, VWC measured from both sensors found 30 to 70 percent of records exceeding 0.45 [fraction], which is above saturation for well-drained soils in the study area. VWC readings were first calibrated using linear coefficients provided for sandy loam soils with saturated electrical conductivity of 0.75 dS/m (Campbell Scientific Inc., 2020). VWC at FC, WP, and saturation (SAT) for the dominant soil type at the field site were estimated using pedotransfer functions (Saxton and Rawls, 2006). These VWC indicators were used as a guideline for manually calibrating CS616 readings. The final correction decreased the offset by a factor of 2. The offset correction was applied to all soil water content data from 2018-2020.

The *a* and *b* constants listed in Table 2.2 were estimated based on empirical values given by Liu et al. for silt loam soils (2006). The *a* constant value lies between soil water contents at FC and SAT for the first day when irrigation was applied. The possible range of *b* constant values were more difficult to determine, as this constant relates to soil drainage rate. Liu et al. gives a general guideline for estimating *b* for silt loam soils, where $b < -0.0173$ for quick draining soils and $b > -0.0173$ for slow draining soils (2006). The range of uncertainty in *b* for both calibration and validation processes were based on $b \approx -0.0173$.

Lastly, the model assumed homogenous soil properties for the entire root zone. Soil water content at FC, WP, and SAT as estimated from layer 1 soil texture properties were applied to all three soil layers. This also includes soil-tension coefficients A and B estimated for layer 1 (see Table 2.2). The following table lists the soil parameters used as input for model calibration and validation.

Table 2.3 Soil Parameters used for Model Calibration and Validation.

Soil Parameter	Value	Unit
θ_{SAT}, all layers	0.39	Volumetric water content [fraction]
θ_{33}, all layers	0.238	
θ_{1500}, all layers	0.119	
A, all layers	0.0114	Unitless
B, all layers	5.556	
$SWC_{(i)}$, layer 1	Observed $SWC_{(i)}$	[mm]
$SWC_{(i)}$, layer 2	SWC at θ_{33}	
$SWC_{(i)}$, layer 3	SWC at θ_{33}	

Actual ET Data

Actual evapotranspiration (ET_a) was calculated for the Harney Basin alfalfa site using turbulent flux data collected from an eddy-covariance tower located at the center of the irrigation pivot. The eddy-covariance tower includes CSAT3 Sonic Anemometer (Campbell Scientific Inc., Logan, UT, USA), and LI-7500DS Analyzer (LI-COR Biosciences, Lincoln, NE, USA), which were installed two meters above ground surface. The sensors were oriented in the predominant wind direction to measure a representative footprint for the 120-acre alfalfa field. EdiRe software package (Campbell Scientific Inc., 2008) was used to calculate latent energy flux (LE) from the turbulence data. Post-processing of latent energy (LE) data included outlier filtering to remove points greater than 600 W/m^2 and less than -100 W/m^2, which represented 5% of total records. A linear interpolation method was used for gap filling removed data points. 30-minute LE was converted to ET (mm) and summed for a daily time step.

Irrigation Schedules

Irrigation records and alfalfa cutting dates provided by the farm manager were used to approximate an irrigation schedule for years 2018-2019. For 2020 irrigation schedule, only monthly pumping records were available through Oregon Water Resource Department. (*https://apps.wrd.state.or.us/apps/wr/wateruse_query/, Accessed June 2020).* A 3-day irrigation schedule was assumed for the alfalfa field based on observed soil water content (SWC) data. This schedule assumes the center pivot makes a full rotation about every 3 days. The cumulative total depth of irrigation a center pivot might apply on a 3-day schedule was estimated. This estimated cumulative total depth was applied in full every third day within the model for 2018-2020 irrigation schedules.

Two different application systems were employed at the alfalfa site; low-elevation spray application (LESA) and mid-elevation spray application (MESA) were used on six and two center pivot spans, respectively. These systems describe nozzle height placement for sprinkler irrigation. MESA systems are widely used on pivot systems in Idaho, and are typically designed with nozzle heights 5-7 ft (1.5 – 2 m) above soil surface. LESA systems are an alterative design that lowers the nozzle height to about 1-2 ft (0.3 – 0.6 m) about soil surface. The LESA design allows water to spend less time in the air and reduce water losses due to wind and evaporation. LESA systems were installed with nozzle spacing 60 in (1.5 m)

apart with nozzles 12 in (0.3 m) from the soil surface. MESA systems were installed with 120 in (3 m) nozzle spacing with nozzles 48 in (1.2 m) from soil surface (M. Owens, personal communication, 2018).

The DI model accounts for "application efficiency" of irrigation systems when calculating the daily water balance (see Table 2.1, Eq. 2.10). Application efficiency (AE) is a measure of the amount of effective irrigation being applied by a system. AE is defined as the amount of water stored in the root zone over the volume of irrigation delivered to the field (Irmak et al., 2011). Water stored in the root zone relates to water that can be used to meet the crop water demand (ET). LESA and MESA systems are cited with application efficiencies between 85-95 percent and 70-85 percent, respectively (Liang et al., 2019). For simplifying model calibration and validation, the efficiency was set at 75 percent since the alfalfa field largely employed the MESA system.

Model Metrics

A two-sample Kolmogorov-Smirnov (KS) test was the primary metric used to evaluate model calibration and validation performance. The two-sample KS test is a nonparametric statistic that compares the two empirical cumulative distribution functions (CDF) by quantifying the distance between them. The DI model simulates SWC for the first and subsequent soil layers. The calibration procedure uses observed SWC as the "reference distribution" to compare to the simulated SWC distribution in layer 1. The null hypothesis (H_o) states the simulated and reference data are drawn from the same probability distribution. H_o cannot be rejected if the KS test p-value is greater than the significance level. The two-sample KS test, "kstest2" function within Matlab (The Mathworks Inc., 2020) was used to test distributions at a 5% significant level.

The model is primarily focused on simulating soil moisture flux from irrigation events, thereby evaluating the contribution of DI from irrigated agriculture. These irrigated periods are visually different from non-irrigated or "dry" periods, which correlate to when irrigation is shut off to allow alfalfa to dry before harvest. The KS test was isolated to testing observed and simulated SWC distributions during irrigated periods. To isolate irrigated and dry periods for the KS test, an index was calculated by taking the absolute square-difference of a 3-day moving average of observed SWC. Dry periods were indexed when these adjusted values

were $\leq 1 \times 10^{-05}$. Values outside of the dry index were used for the irrigated index (Figure 2.6).

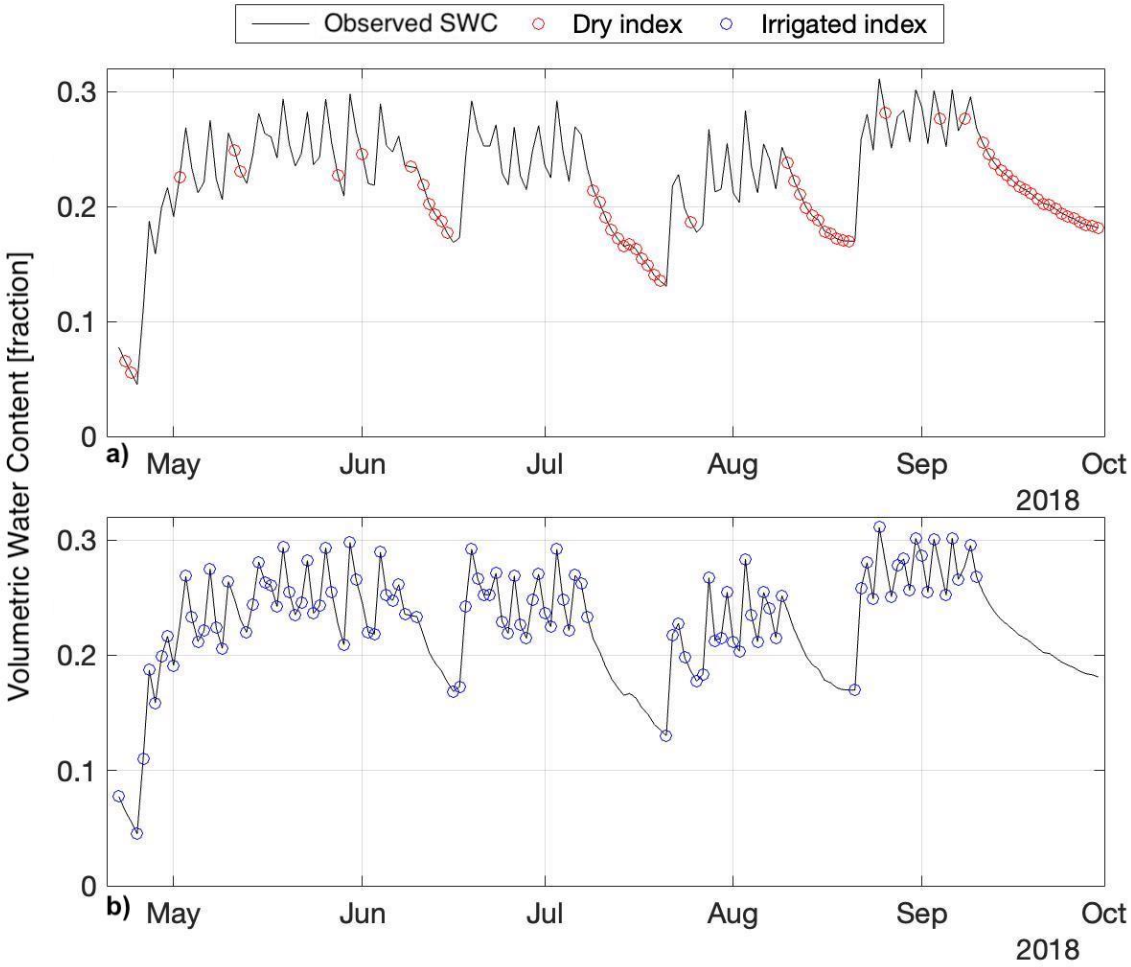

Figure 2.6 Dry and Irrigated SWC Index for KS Test. The index shown is for 2018 observed SWC data that was used for model calibration metrics (KS test).

Results and Discussion

The following sections present results for model calibration using 2018 field data, and model validation for 2019-2020 data collected at the same alfalfa field in the Harney Basin, Oregon. SWC was simulated for three soil layers, each layer testing an uncertainty range for *a* and *b* drainage parameters (see Table 2.2). "Successful" model runs were determined when simulated SWC in layer 1 was found to be from a statistically similar distribution as observed SWC using the KS test. Soil layers 2 and 3 were not calibrated due to limited soils data.

Model calibration with 2018 data

The first soil layer of the DI model was calibrated using forcing parameters of observed SWC and ET_a. An irrigation schedule based on farm records was used to estimate a three-day irrigation schedule. Drainage parameters *a* and *b* were tested over a range of uncertainty until the simulated SWC for layer 1 was statistically similar to observed SWC. Successful model runs resulted from an input range of (0.33, 0.35) for parameter *a* and a range of (-0.20, -0.25) for parameter *b.* Each input range tested 10 parameter values, which resulted in a total of 100 model runs. From these 100 model runs, 32 runs failed to reject the null hypothesis for the KS test; in other words, simulated SWC for layer 1 was drawn from the same probability distribution as the observed SWC.

Figure 2.7 shows simulated SWC for layers 1-3 for a successful calibration run. Cumulative seasonal DI from this model run was 126 mm. This DI represents about 20% of applied irrigation, which was estimated from a fixed application efficiency (AE) of 75%. Thus, the total inefficiencies resulting from DI and losses attributed to irrigation system AE are 45% of total on-farm irrigation delivery. Other successful runs showed cumulative seasonal DI from 115 – 135 mm. Since model calibration was simplified by assuming an AE of 75%, it is likely DI and overall farm efficiency would change if an uncertainty range for AE was included.

Challenges that arose during model calibration were mainly due to narrowing the range of tested values for the *a* and *b* parameter used for Eq. 2.1 (see Table 2.1). Initially tested *b* parameter values were based on empirical values provided for silt loam soils (Liu et al., 2006). Values found to successfully calibrate the model were more than one order of magnitude greater than those provided. This means the soils observed at the alfalfa field are classified as fast draining soils (Liu et al., 2006). One explanation for the large difference in *b* parameters are simply due to soil texture or structure at the surface layer. It is also possible preferential flow increased the rate of drainage at the upper 30 cm of soil. Narrowing the range of realistic *a* parameter values also presented challenges. Ultimately, the *a* parameter represents SWC on the day of irrigation application. Irrigated soils show water contents between saturation and field capacity roughly 1-2 days after application. For soils found at the Harney Basin alfalfa site, VWC at FC and SAT were estimated as 0.39 and 0.23 [fraction], respectively. These were determined using pedotransfer functions (Saxton and Rawls, 2006). The *a* parameter values found to successfully calibrate layer 1 of the model were between 0.33 and 0.35, demonstrating

that the *a* parameter was closer to estimated SWC at saturation.

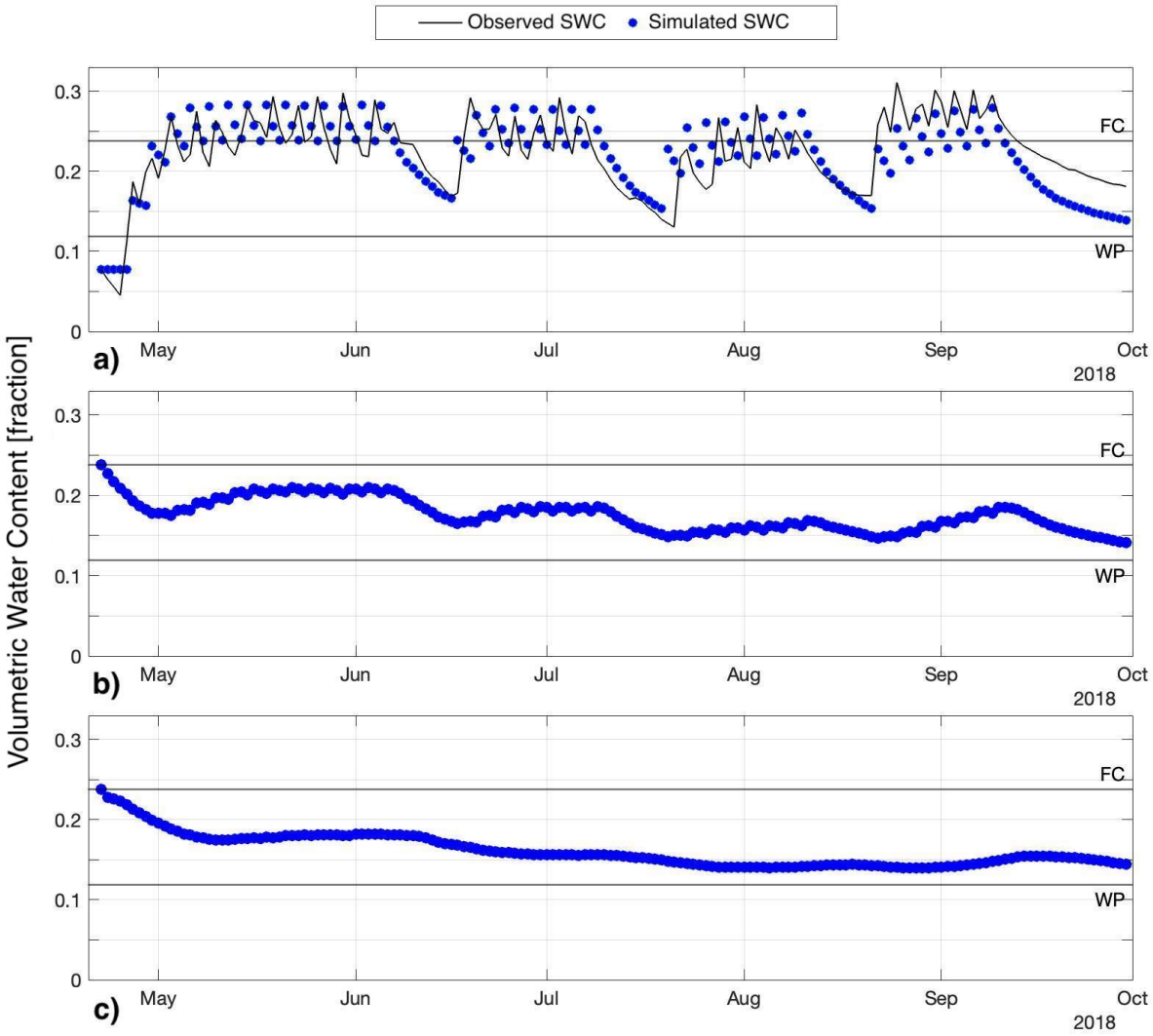

Figure 2.7 Successful Calibration Run Using 2018 Observed SWC. Graph a) shows layer 1 which was calibrated with in-situ soil data. Graph b) and c) show simulated SWC for layer 2 and 3, respectively.

Figure 2.8 shows the accompanying soil water balance for the calibrated model run in Figure 2.7. Cumulative seasonal DI represents all infiltration from layer 3 of the model, which is the bottom boundary layer of the root zone. The temporal distribution of DI show greater amounts at the start of the irrigation season which decrease over the warmer months (Figure 2.8, graph c). For semi-arid climates receiving precipitation mainly in the off-season, this suggests irrigation efficiency could improve at the beginning of the season by relying on antecedent SWC. Layer 2 and layer 3 were modeled using initial SWC at field capacity, which might be typical of a "wet winter" that results in enough precipitation to fill deeper soil water storage.

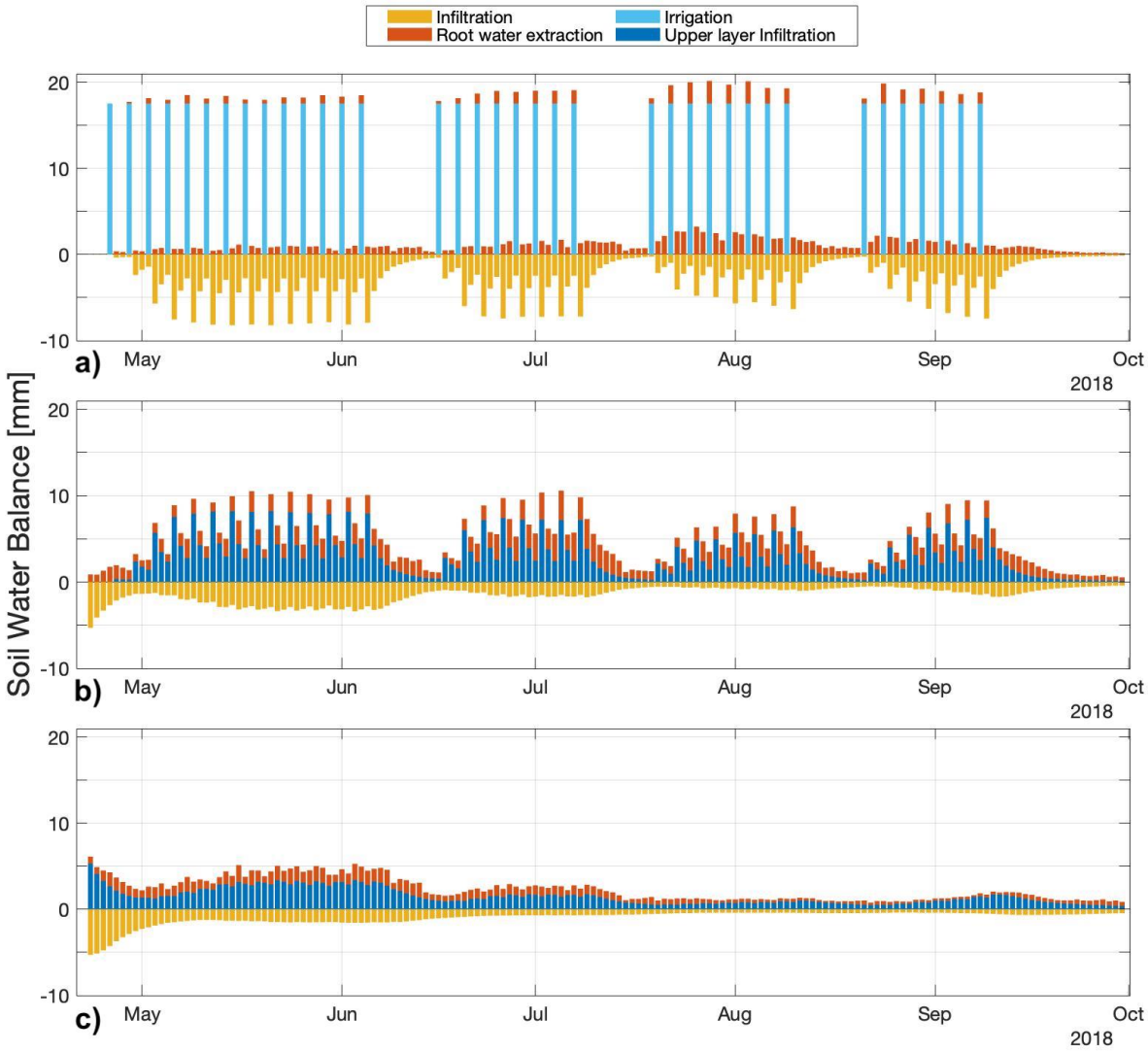

Figure 2.8 Soil Water Balance for Calibrated Model Run in Figure 2.7. Graph a), b), and c) represent soil water balances at layer 1, 2, and 3, respectively. Light blue bars represent applied irrigation for layer 1. Darker blue bars represent infiltrated soil moisture from the overlying soil layer.

Model performance for 2019-2020 data

Once the calibration process established a successful input range for drainage parameters *a* and *b*, simulated SWC for layer 1 was tested using observed SWC for 2019-2020 at the same field site. The established input ranges from calibration were used to test model performance, while also including year-specific forcing parameters to guide model output (observed SWC, ET_a, and irrigation schedules).

The model was successful at simulating layer 1 SWC for 2019-2020. The success rate for 2019 model runs was about 40 out of 100 model runs. Successful runs for 2020 data were comparatively few, with only 3 out of 100 runs. The observed SWC time series for 2019-2020 were notably different from that of 2018 (Figure 2.9 and Figure 2.10). 2018 observed SWC shows sharp "peaks" which are clear indications of large water flux typical of a well-irrigated field (see Figure 2.7). The observed SWC for 2019 and 2020 show dampened peaks, especially evident for 2019 in late May. These dampened peaks correspond to the farmer's records, where irrigation was turned off about May 4 due to rain and not turned on until June 20. For 2020 observed SWC, an irrigation record was not provided, so it is unclear whether scheduling included rainfall events. It is possible that as the years progressed, soil moisture sensor measurements were compromised due to a variety of factors that can occur over the span of three years. These factors include soil compaction from farm management, sensor drift, or changes to electrical conductivity due to salination.

Tests of model performance with subsequent year soils data highlight one principal characteristic of the DI model; the model focuses on simulating soil water content for *irrigated* crops. Irrigated soil systems reflect consistent soil moisture patterns typical of irrigation scheduling. The model can effectively capture these patterns by relying on analytical solutions to estimate soil drainage. When observed SWC exhibits natural variation due to rainfall events or other dominant factors that affect soil drainage, such as vegetation and soil properties, an analytical solution may not be as affective in simulating SWC. Additionally, in these regions with sparse rainfall, some farmers might forego irrigation if a significant rainfall event occurs. The DI model did not account for rainfall events, though this could be done by adjusting the irrigation schedule.

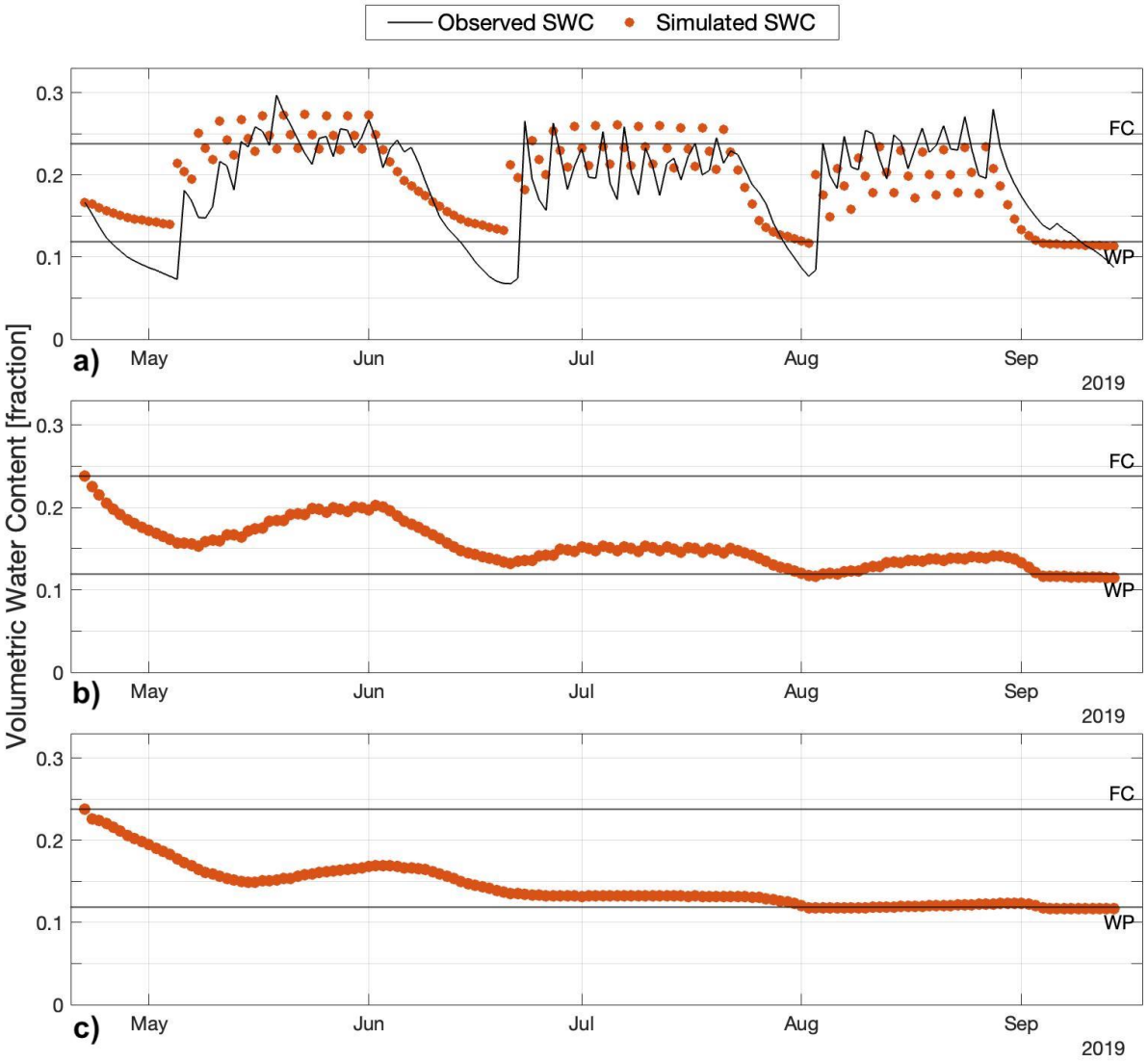

Figure 2.9 Model Performance with 2019 Observed SWC. Graph a) shows simulated SWC for layer 1 which was tested against observed SWC for 2019. Graph b) and c) show simulated SWC for layer 2 and 3, respectively.

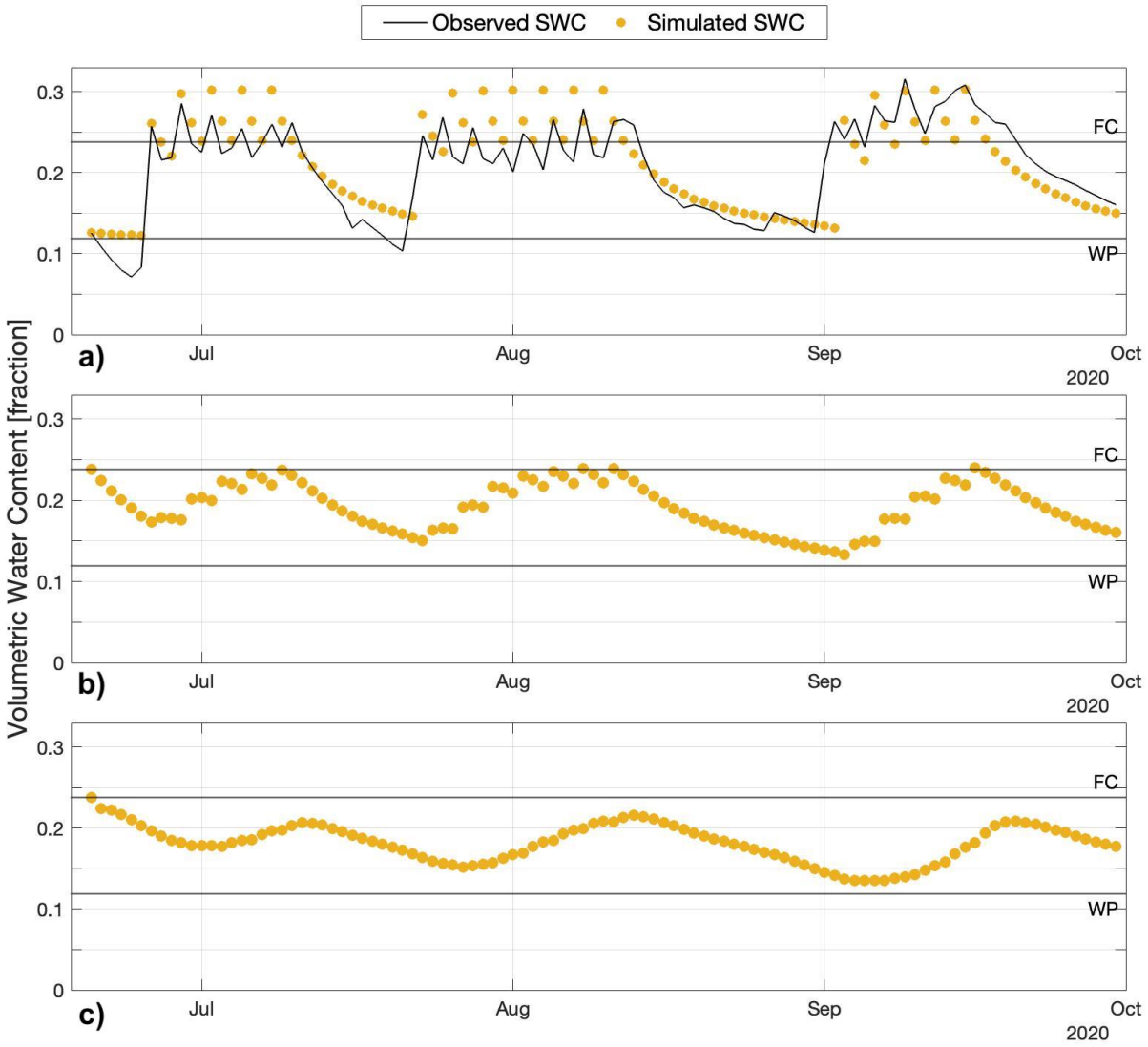

Figure 2.10 Model Performance with 2020 Observed SWC. Graph a) shows simulated SWC for layer 1 which was tested against observed SWC for 2020. Graph b) and c) show simulated SWC for layer 2 and 3, respectively.

Figure 2.9 shows simulated SWC based on input parameters for 2019 data. These data include actual ET, which is partitioned into a root water extraction (RWE) value for each soil layer. RWE is a function of soil water stress, soil layer depth, and a relative distribution of root mass within the root zone. The effect of this function becomes apparent towards the end of the growing season in 2019 when SWC for all layers approaches wilting point. A conditional statement for model validation runs states that when SWC $\leq$ WP , no RWE should be taken from the layer. This conditional statement supports the definition of wilting point, which is the point at which water cannot be extracted by the plant due to low soil water

potential. In terms of the conservation of energy, ET_a must be accounted for in modeling the irrigated system as it is an actual measured value. In this case, ET_a can be attributed to soil evaporation only. Whether this is a valid statement relies on whether the soil moisture data represents real conditions. 2019 observed SWC showed greater "drawdown" periods when irrigation was turned off and the soil was allowed to dry. Before irrigation was turned on, SWC for 2019 had dried down to about 0.08 VWC. This is a difference of about 0.02-0.07 VWC as compared to 2018 and 2020 data. As will be shown in Chapter 3, 2019 demonstrated drier climatic conditions in southern Idaho that resulted in higher actual ET. It is likely Harney Basin also experienced drier climatic conditions for 2019, which would explain why drawdown periods were greater for this time series.

Challenges arising from model performance tests were largely due to unrepresentative observed soil moisture data. The time series of observed SWC for 2020 was shortened to between July and October to isolate periods of observed SWC realistic for irrigated soils. When irrigated and non-irrigated periods could not be distinguished from observed soil moisture data, it was difficult to assign an irrigation schedule. 2020 presented greater difficulty since farm records were not given and monthly pumping records were used to approximate applied water. The irrigation schedule and subsequent model results for 2020 performance runs should be viewed with caution, since they do not agree with earlier model findings. For instance, cumulative seasonal DI estimates for 2020 runs were about two times greater than values found for 2018-2019, with values around 260 mm. Another challenge of testing model performance is evaluating representative SWC simulated for lower layers. A promising feature of the model is it shows attenuation of SWC with greater depths, as typical for in-situ soil moisture data. Future development of this model will seek opportunities to use multi-depth soil moisture data to test model performance for deeper layers.

Chapter 3: Magic Valley Deep Infiltration Study

Water resource accounting continues to be a critical part in managing water shortages of today and in the future. Similar to a person's checkbook, water accounting keeps a record of inflows and outflows to a hydrologic system, from the spatial scale of an agricultural field to that of a drainage basin. Water is almost always moving in both time and space, which creates a challenging task for water resource managers. Additionally, the methods to measure certain changes in water, like groundwater recharge and evapotranspiration, are not always accessible, easy to interpret, or simple to explain to the community at large. Finding solutions to these difficult tasks of water management are crucial with current and forecasted droughts worldwide.

With a high demand on freshwater resources and irrigation being the largest global consumer of these resource, policy makers are focusing on ways to encourage water conservation in the agricultural field. Conservation efforts in the agricultural field are intended to make water more available to other users, such as industrial or domestic. In the past decade, water policy has sided in favor of improved irrigation technology. These policies provide subsidies to farmers to update older irrigation methods in favor of systems with improved irrigation efficiency (IE). Contrary to the goals of these policies, in many cases the adoption of improved IE systems has increased water consumption per acre (Perry and Steduto, 2017). It was also found these pre-existing "inefficiencies" were indirectly supporting other water users through aquifer recharge (Stewart-Maddox et al., 2018) or downstream flows (Ward and Pulido-Velazquez, 2008). In order to make water available for other uses in a watershed or a basin, it is suggested a closer evaluation of irrigation's "nonbeneficial uses" be performed (Grafton et al., 2018). "Beneficial use" is a legal description associated with water rights. In the case of irrigation water rights, water is considered beneficially used if it goes towards growing something planted. Nonbeneficial uses describe water that is not directly used in plant growth as measured through plant evapotranspiration (ET). In this study, deep infiltration (DI) describes one nonbeneficial use of water in irrigated systems, where applied water exceeds the holding capacity of the root zone and is lost to deeper groundwater. It should be noted that DI can have certain "benefits" for farmers and other water users, such as aquifer recharge and soil desalination, though here DI is nonbeneficial use in context of in-farm water efficiency.

When it comes to developing and adopting irrigation technology with higher IE, the main motivation is to reduce water losses that occur between a pressurized irrigation system and the soil surface. For instance, conventional center pivot systems with high-impact sprinklers demonstrate a large, wetted radius, though have high losses due to wind drift, canopy interception, and evaporation (Peters et al., 2019). Modified systems, such as Low Energy Precision Application (LEPA) were recommended as early as 1978 to reduce water and energy consumption (Lamm and Porter, 2017). Variations of the LEPA system, such as Low Elevation Spray Application (LESA), are widely practiced in the Southern Ogallala Aquifer Region to reduce groundwater withdrawals (Colaizzi et al., 2009). These systems modify the required pressure and the distance of the sprinkler head from the surface to reduce water losses to wind drift and evaporation. Another added benefit from operating an irrigations system at lower pressure is increased energy savings.

With modified sprinkler systems continuing to be tested across the Pacific Northwest and promoted for basin-wide water savings, this study calls for a closer evaluation of the application efficiency (AE) of such systems. AE is defined here as the ratio of water delivered directly to the root zone of the crop, over the water that is delivered to the application system (Irmak et al., 2011). Not only does AE evaluate losses that are more apparent above the soil surface, such as wind loss or evaporation from canopy interception, but losses that could occur below the surface due to deep infiltration. The reality is that deep infiltration does occur from irrigated lands at a scale and frequency large enough to be detected through aquifer recharge (Stewart-Maddox et al., 2018). Aquifers are an important freshwater reservoir for agriculture and are continuing to be depleted at a rate that exceeds natural recharge. The implications of irrigation-induced recharge and water "savings" from improved irrigation efficiency makes this study relevant today.

Background on Study Area

This study focuses on the south-central region of Idaho known as the Magic Valley. This region is one of the most agriculturally productive regions in the state and in the Northwest United States. The area was "magically" transformed during the early 20th century from desert to cropland, with the construction of canal systems and the Milner and Minidoka Dams. Today, the agricultural industry continues to be the primary economic

resource for local communities and the state. Forage crops like alfalfa are grown in the Magic Valley and support Idaho's dairy industry, which accounted for $2.4 billion in farm cash receipts in 2019 (Ellis, 2019). Additionally, the valley overlies a portion of the Eastern Snake River Aquifer, which has been a chief source of water and key factor in Idaho's economy and agricultural production.

Within the past few decades, concern has been placed on the Eastern Snake River Aquifer due to declining groundwater levels. Groundwater levels have been declining since the 1970's, which can be attributed to the conversion of flood irrigation to pressurized systems, increase in the number of groundwater withdrawals and overall growth in the area (Stewart-Maddox et al., 2018). The effect of irrigated agriculture on groundwater resources has highlighted the connectivity of surface water and groundwater in southern Idaho. As such, water resource management and administration of water rights in the state has evolved to collectively manage surface water and groundwater.

With the agricultural sector supplying about 42 percent of jobs and 59 percent of total sales in the Magic Valley (Ellis, 2021), efforts in agricultural water accounting will help evaluate long-term water security and economic prosperity for the region. This study will apply the DI Model described in Chapter 2 over the Magic Valley area to estimate near-surface DI from irrigated farmland. The primary goal is to evaluate DI losses from pressured irrigation systems with improved efficiency. The area has been transitioning to pressured irrigation systems since the 1950's, with more recent adoption of modified systems like LEPA and LESA. This study has relevance in regional water balance estimates and the collective management of surface water and groundwater in southern Idaho.

Methods

The following describes methods used in creating test scenarios for the Magic Valley Deep Infiltration study. Test scenarios were based on irrigated alfalfa for two different climatic conditions and three different soil types applicable to the region. The "climatic conditions" include input variables that account for the atmospheric demand for water as well as antecedent soil moisture from winter precipitation. Three irrigation schedules were tested over these soil types to evaluate differences in management for pressurized irrigation systems.

Study Area and Irrigated Alfalfa

Evaluation of deep infiltration for the Magic Valley was limited to irrigated alfalfa found in six counties, namely Gooding, Lincoln, Jerome, Minidoka, Twin Falls, and Cassia. Alfalfa was selected for two reasons; firstly, the model was calibrated against in-situ soil moisture data from an alfalfa field, and secondly, alfalfa is a primary forage crop that supports the dairy industry in the Magic Valley. Alfalfa has also been shown to be resilient to deficit irrigation practices, which has relevance in adaptive strategies for regions facing water shortages. Most alfalfa production occurs in proximity to the Snake River, which runs along the northern border of Twin Falls and Cassia counties. Growing conditions around the Snake River are likely to be affected by waterbody-induced microclimates, which have a cooling effect on the local air temperature as well as an increase in relative humidity. This phenomenon is also true for irrigated croplands, which increase the amount of moisture in the air and create a cooling effect for the surrounding area. Thus, weather data used for the crop ET function (Eq. 2.9) was focused on local weather stations near the Snake River, or generally surrounded by irrigated farmland.

Magic Valley counties were masked for irrigated alfalfa using a spatial layer for alfalfa crops for 2019, which was provided by the United States Department of Agriculture-National Agricultural Statistics Service (USDA-NASS) (*https://nassgeodata.gmu.edu/CropScape/, Accessed June 2021*). This raster layer was overlain with a vector layer describing irrigated lands for 2015 (Idaho Department of Water Resources, *https://data-idwr.opendata.arcgis.com /pages/gis-data/, Accessed June 2021*). This step was performed to ensure alfalfa was irrigated only, and to provide a polygon layer for other spatial analyses done in ArcGIS 10.5 (Esri Inc., 2021).

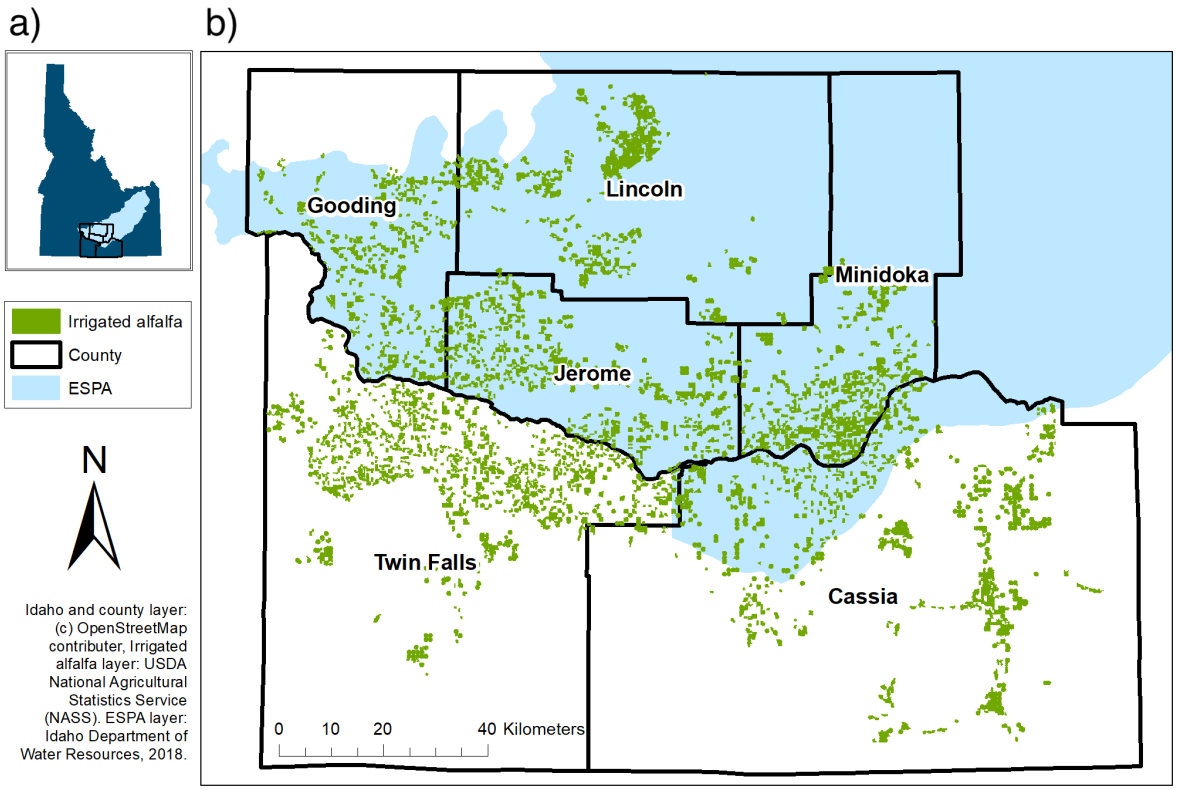

Figure 3.1 Magic Valley, ID Irrigated Alfalfa. Shown in green is irrigated alfalfa for 2019 (USDA-NASS crop data layer). Figure a) shows the Magic Valley as located in the State of Idaho, as well as the primary aquifer, the Eastern Snake Plain Aquifer (ESPA, in blue).

Test Scenarios

The model requires two main input variables that account for major soil water fluxes in the root zone, namely, crop ET (ET_c) and an irrigation schedule. Other user-defined parameters, including soil texture and drainage constants (Equation 2.1) were based on three dominant soil types identified for Magic Valley soils in which alfalfa was grown. Three irrigation schedules were created to evaluate the effect of farm management on deep infiltration. Variations in climatic conditions were accounted for by altering the atmospheric demand (i.e., ET_c) and the initial soil water content. The atmospheric demand for water has relevance to climate change, since crop evapotranspiration is partly influenced by increased air temperatures. Climate change can also alter the availability of water. This has implications for semi-arid climates that receive precipitation predominantly in the off-season. Altering the initial SWC partially accounts for changes in water availability attributed to climate change.

Table 3.1 Magic Valley DI Study Test Scenarios. 36 scenarios were created to represent a range of growing conditions for Magic Valley irrigated alfalfa. 18 scenario descriptions are listed below for simplicity, where each scenario was tested under two ET_c time series (ET1, "dry" and ET2, "wet").

Scenario No.	Initial SWC (Layers 1-3)	Irrigation Schedule	Soil Type (Layers 1-3)
1	Wet	One-day	Well-drained
2	Dry		
3	Wet	Two-day	
4	Dry		
5	Wet	Three-day	
6	Dry		
7	Wet	One-day	Poor-drained
8	Dry		
9	Wet	Two-day	
10	Dry		
11	Wet	Three-day	
12	Dry		
13	Wet	One-day	Excessive-drained
14	Dry		
15	Wet	Two-day	
16	Dry		
17	Wet	Three-day	
18	Dry		

Scenario Data for DI Model

Reference ET and Crop Coefficient

In order to estimate crop evapotranspiration within the DI model, reference ET (ET_r) and a crop coefficient (Kc) time series are required inputs. ET_c is a function of weather conditions, crop type, as well as management and environmental conditions, and can be estimated through the crop coefficient method (Allen et al., 1998). This method first requires calculating ET_r, which accounts for climatic conditions that govern the rate of evaporation. It is based on a crop reference surface that is uniform in height and well-watered so only climatic factors are considered (Allen et al., 1998). The second component of estimating ET_c is the crop coefficient, which describes the difference in evapotranspiration between the reference crop and another crop type. In other words, Kc is the ratio of crop ET over that of the reference ET, as shown below:

$$Kc = \frac{ET_c}{ET_r} \quad \text{Eq. 3.1}$$

Kc fluctuates throughout the year largely as a function of growth stages. For alfalfa crops, this includes periodic harvest. The model incorporated three harvests into the Kc time series as typical for southern Idaho farm management.

The following describes methods used to determine two ET_r and Kc time series, which are broadly described as "dry" and "wet" growing seasons. These terms describe general climatic factors that can influence crop ET for any given year. For "dry" growing seasons, the calculated ET_r is higher due to increase solar radiation, wind, and high air temperature. These weather conditions increase the amount evapotranspiration. "Wet" growing seasons show comparatively lower ET_r due to increased humidity. Representative "wet" and "dry" year ET were determined for irrigated alfalfa in the Magic Valley by using gridded maps of actual ET (ET_a) provided by Idaho Department of Water Resources (IDWR) (*https:/data-idwr.opendata .arcgis.com/pages/gis-data, Accessed June 2021*). These ET_a maps are generated using the METRIC model, which estimates ET_a as a residual term from a surface energy balance calculated from 30-meter Landsat images (Allen et al., 2011). Each instantaneous Landsat image used in METRIC is assigned a pixel value (units depth) which is interpolated over time to develop a cumulative ET_a map for the length of the growing season (3/1 – 10/31).

ET_a for years 2009-2019 was tabulated for areas growing alfalfa within the Magic Valley. IDWR ET_a maps for 2012 and 2014 were unavailable. Maps were masked for alfalfa using the USDA-NASS spatial layer, which were then averaged for each county in the Magic Valley. The county average (n =6) was used towards an overall Magic Valley ET_a average for 2009-2019. This process allowed for a comparison of actual ET from alfalfa for a ten-year span (see Figure 3.2). IDWR maps use remote sensing methods that allow detection of water shortages and plant stress that are missed by using the crop coefficient method (Allen et al., 2011). Tabulating actual ET helps identify interannual variation due to climatic conditions as well as overall management practices for alfalfa in the region.

To account for two distinct time series related to the atmospheric demand for water, years 2015 and 2019 were chosen to represent the "dry" and "wet" growing seasons, respectively. Corresponding reference ET time series for years 2015 and 2019 were chosen from Agrimet weather stations in the Magic Valley. Agrimet is a climate data network

provided by the Bureau of Reclamation (USBR), which includes a few stations located within the Magic Valley. Daily reference ET was downloaded for 2015 and 2019 from Twin Falls (Kimberly) Agrimet station, for dates between April 1 and October 9. The Kimberly Agrimet station was selected due to its location within the Magic Valley and its proximity to irrigated cropland in all directions.

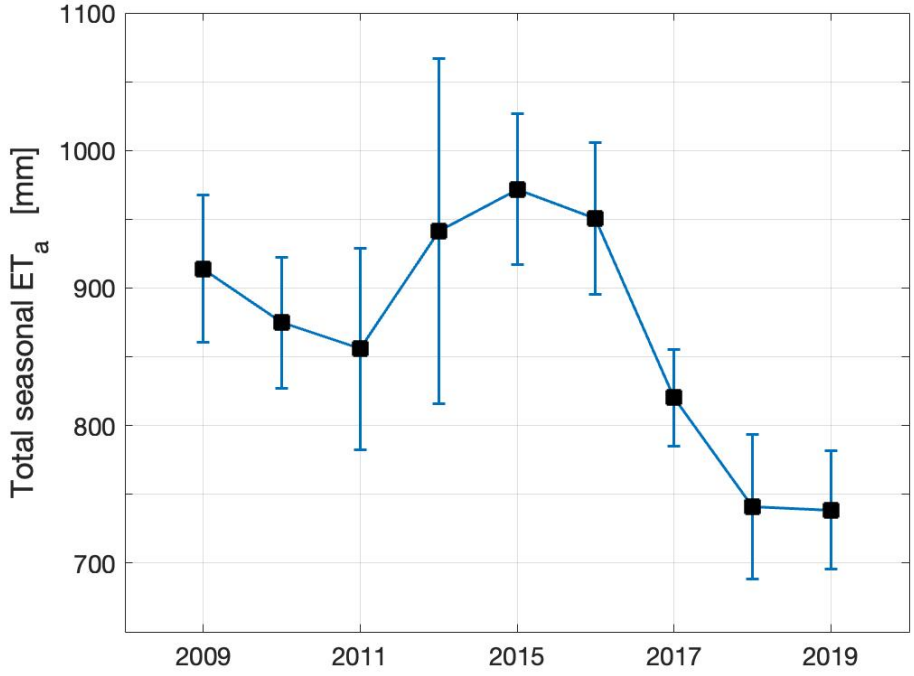

Figure 3.2: Total Seasonal ET_a for Magic Valley Alfalfa. Total seasonal ET_a (Mar 1– Oct 31) for alfalfa was averaged for 6 counties within the Magic Valley. The Magic Valley county average is shown in here, with standard error in blue. Years 2012 and 2014 are excluded.

Finally, two crop coefficient (Kc) time series corresponding to "wet" and "dry" growing seasons were developed. As mentioned in Equation 3.1, the crop coefficient (Kc) can be described as the ratio of ET_c over that of the ET_r. The reference ET represents a theoretical ceiling of evapotranspiration rate by a crop, with the assumption the crop is well-watered and disease free. The calculated crop ET will not always reach this ET rate due to growth stages, health, and environmental factors affecting the plant. Limiting factors preventing full potential ET also include atmospheric conditions, for example, when less solar radiation is received at the surface or when relative humidity is high.

The approach used in this model to create Kc time series was to take the ratio of Magic Valley average ET_a (Figure 3.2) over the ratio of cumulative total daily ET_r retrieved from the Kimberly Agrimet station. This ratio is similar to a crop coefficient, though it is used here to broadly estimate an average ET_a / ET_r relationship for the entire Magic Valley for years 2015 and 2019. This ratio was used to adjust each year's Kc time series until the area above the ET_a / ET_r ratio line is equal to the area below. Three alfalfa harvests were incorporated into the Kc time series (Figure 3.3).

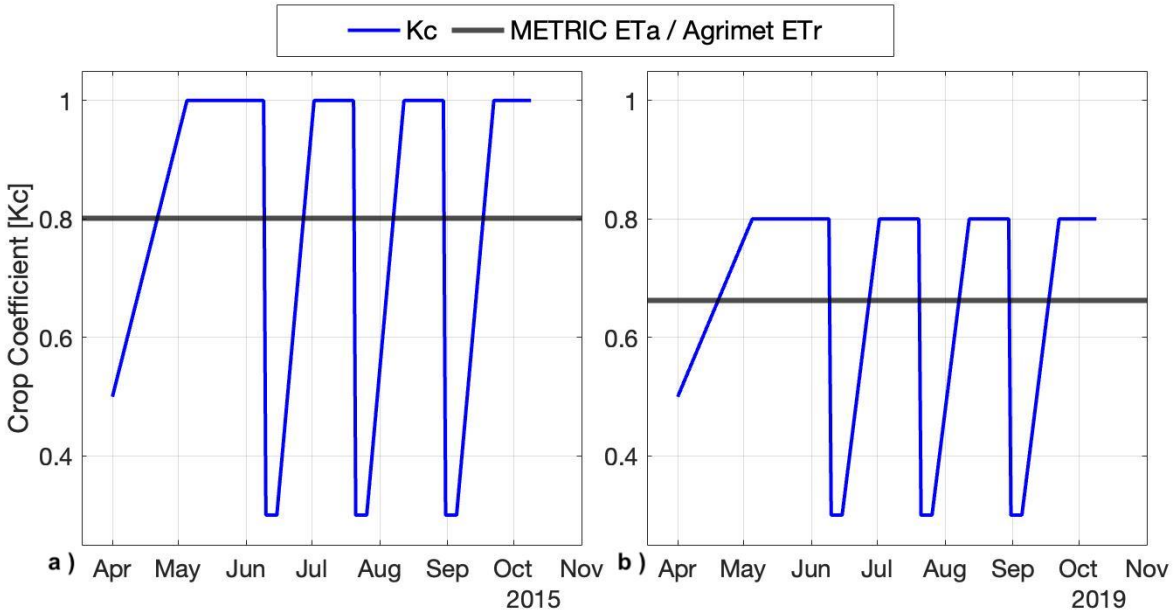

Figure 3.3 Crop Coefficients for "Dry" and "Wet" Growing Seasons. 2015 is shown in graph a) which represents Kc during the "dry" season. Kc for 2019 is shown in graph b) and represents the "wet" season. The "dry" season shows full potential ET where Kc = 1. The "wet" Kc time series illustrates low atmospheric water demand where Kc reaches a maximum at 0.80.

Irrigation Schedule

Three center pivot irrigation schedules with different application rates were created for the Magic Valley test scenarios. Application rates for sprinkler systems are functions of both system design, including flow rate and nozzle type, as well as the operating speed of the system. Typical center pivot systems for southern Idaho are designed to apply water at flow rates from 6.5-7.5 gallon/minute/acre (Hines and Neibling, 2013). The application rate for center pivots can be controlled with a percent timer, which adjusts the motor speed of the last tower. Faster speeds are used to apply less water to the ground, where slower speeds increase the depth of water per revolution.

A few factors may be considered by an irrigator when setting the pivot speed. First, speed may be decreased to apply more water than the crop water requirement (ET). This is typically done to supplement water lost through application inefficiencies. A second consideration in choosing a pivot speed is the infiltration rate (IR) of the soil. If a soil has a low IR, then applied water could either become runoff or cause pooling at the surface. The latter condition contributes to the non-consumptive water loss (evaporation), or also causing wheel track rutting and preventing the pivot from moving freely. Ideally, the irrigator will be able to schedule the pivot to apply sufficient water to meet the ET requirement, limit plant stress, and avoid excess runoff or standing water. The irrigator considers the time it takes for the pivot to make one revolution, and at what depth water is applied over that time. Irrigation schedules were based on one-, two-, and three-day pivot revolutions. An average application rate of 0.0133 in/hr for a 6 gallon/minute/acre flow design was used to create these schedules (Leib and Grant, 2019). Though center pivot systems apply water daily as they rotate around the field, these schedules apply the cumulative total depth on the scheduled day. In retrospect, this approach does not consider evaporative losses that happen on a diurnal cycle. For instance, a one-day irrigation schedule wets the surface more often compared to a three-day schedule. Still, evaporative losses from soil are likely minimal when estimating DI for a regional water balance. Table 2.3 summarizes the irrigation schedules and their application rates. Application depth was 120 cm for all schedules, which is the amount of water delivered to the application system. These schedules were tested against all soil types (i.e., poorly-drained, well-drained, excessively-drained).

Table 3.2 Irrigation Schedules used in Magic Valley Test Scenarios

Irrigation schedule	Speed description	Application rate
Every day	Fast speed	0.32 in/24-hrs
Every two days	Medium speed	0.64 in/48-hrs
Every three days	Slow speed	0.95 in/72-hrs

Irrigation efficiencies were tested from a range of 72-90%, with increasing efficiencies of 2%. Efficiencies are based on application efficiencies (*AE*), or the ratio of water reaching the soil

profile over the amount delivered to the application system. This range of *AE* are based on estimated efficiencies given for sprinkler systems, such as high-pressure impact sprinklers, MESA, LESA, and LEPA systems (Peters et al., 2019).

Magic Valley Soils

Dominant soil drainage classes were identified for agricultural soils in the Magic Valley in which alfalfa is grown. Soil information was retrieved from SoilWeb, an online interactive map providing USDA-NRCS soil survey data. Spatial layers of soils were masked with the irrigated alfalfa spatial layer to identify soils of interest. These "alfalfa soils" were then categorized into three drainage classes (well-, poorly-, excessive-drained), which information is found in the Official Series Description (*https://casoilresource.lawr.ucdavis.edu*/, *Accessed June 2021*). Well-drained soils represented about 84% of alfalfa soils for the Magic Valley, where poor- and excessive-drained soils were about 7-9% (Figure 2.3).

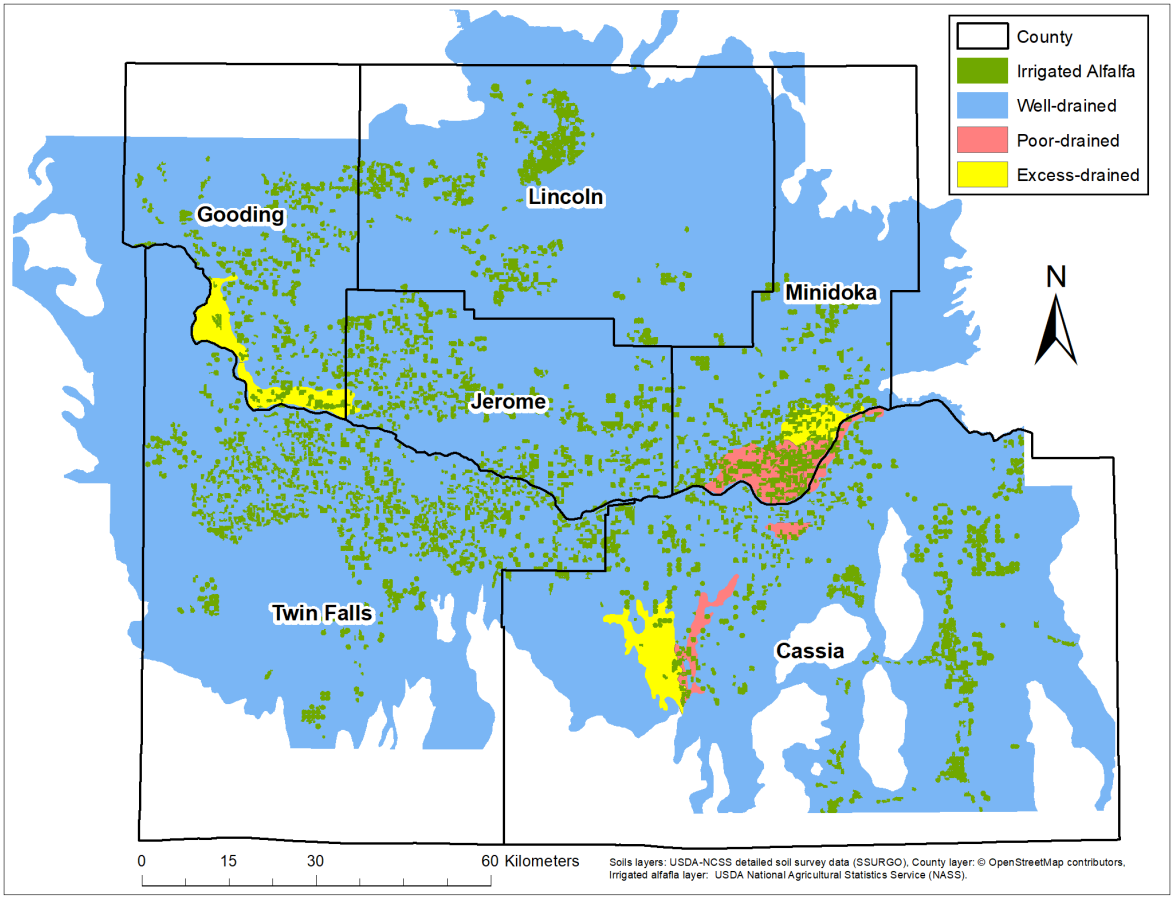

Figure 3.4 Dominant Soil Drainage Classes for Magic Valley Alfalfa. Irrigated alfalfa (in green) was used to mask soils and identify drainage class. Well-drained soils (in blue) were the highest represented drainage class, representing 84% of land in which alfalfa is grown.

Once drainage classes were identified, their corresponding shapefile was exported and used to define the area of interest within Web Soil Survey (*https://websoilsurvey .sc.egov.usda.gov/App/WebSoilSurvey.aspx, Accessed June 2021*). For each soil series categorized under each drainage class, the percent clay, silt, and organic matter was found for a soil depth of 120cm. A weighted average was taken to account for soil series that contributed a higher percent of total acreage. Volumetric water contents (VWC) at SAT, FC, and WP, and A and B parameters for soil-tension were then calculated for each drainage type using pedotransfer functions by Saxton and Rawls (2006). The resulting soil parameters are shown in Table 3.3.

Drainage constants used in Equation 2.1 were estimated for each drainage class based on values found through model calibration. Layer 1 of the model was successfully calibrated

when the *a* parameter lie between 0.33 and 0.35 and the *b* parameter between -0.20 and -0.25. These drainage parameter values describe well-drained soils for data used for model calibration. Since well-drained soils make up the majority for the Magic Valley, a wider range was estimated based on guidelines given by USDA. Assuming well-drained soils reach field capacity around 1-2 days (USDA, 2008), a decay function by Richards et al. (1957) (Eq. 3.2) and SWC at FC were used to approximate parameter *a* and *b*.

$$W = aT^{-b} \quad \text{(Eq. 3.2)}$$

Where W represents water content, T as time, and *a* and *b* are positive constants describing drainage rates for a certain soil type. Poorly- and excessive-drained soils followed the same procedure by using Eq 3.2 and SWC at FC classified for each soil texture. Poorly-drained soils were estimated to reach FC around 2-3 days, where excessive-drained soils reach FC $\leq$ 1 day.

Table 3.3 Soil Parameters for Magic Valley Test Scenarios.

Soil drainage class	VWC at saturation	VWC at field capacity	VWC at wilting point	Soil-tension parameters [A; B]	Equation 2.1 *b* parameter (range)	Equation 2.1 *a* parameter
Well-drained	0.38	0.26	0.10	[0.22; 3.7]	(-0.14, -0.30)	0.30
Poor-drained	0.38	0.18	0.07	[0.034; 4.3]	(-0.12, -0.18)	0.22
Excessive-drained	0.40	0.10	0.05	[0.001; 4.7]	(-0.27, -0.30)	0.14

Results and Discussion

Presented in this section are regionwide estimates of deep infiltration for dominant growing conditions and management for Magic Valley alfalfa. Thirty-six test scenarios (see Table 3.1) were created to show a range of possible values under different types of irrigation schedules, irrigation efficiencies, soil textures, and atmospheric conditions.

Consumptive Use Efficiency

Two metrics used to illustrate the results from test scenarios are the application efficiency (AE) and consumptive use efficiency (CUE). As defined here, AE is the ratio of water applied to the soil and integrated into the rooting zone to the quantity of water delivered to the irrigation system. CUE describes the efficiency of applied irrigation used directly for the consumptive use of irrigation, or ET:

$$CUE = 1 - \sum_{i=1}^{192} \frac{DI_{LYR3(i)}}{IRR_i * AE} \quad \text{(Eq. 3.3)}$$

Where DI_{LYR3} describes all deep infiltration from the deepest root zone boundary (layer 3 in this case) and IRR*AE is the scheduled irrigation multiplied by the application efficiency, respectively. Test scenarios were tested over a course of 192 days from April 1 to October 9. The AE metric is typically used to describe modified pressurized irrigation systems, which focus on losses above the crop surface due to wind and evaporation. CUE is included to describe losses that occur below the root zone to DI.

Figure 3.5 shows the effect of increased application efficiencies on CUE. The figure separates climatic conditions based on color, where red markers indicate growing seasons where atmospheric water demand was high (hereafter denoted ET1), and where atmospheric water demand was low, as shown in blue (ET2). Each marker shape represents a drainage class. The figure is separated into four graphs describing “wet” and “dry” initial SWC. Drainage rates showed a linear relationship on CUE. For simplicity, model runs testing the upper and lower values for parameter *b* (see Table 3.3) are shown in the figure. Well-drained soils had a larger range for drainage rate, which is reflected in a larger range of CUE values. A one-day irrigation schedule is shown; changes in CUE due to irrigation schedules were within 1 percent for all soil types.

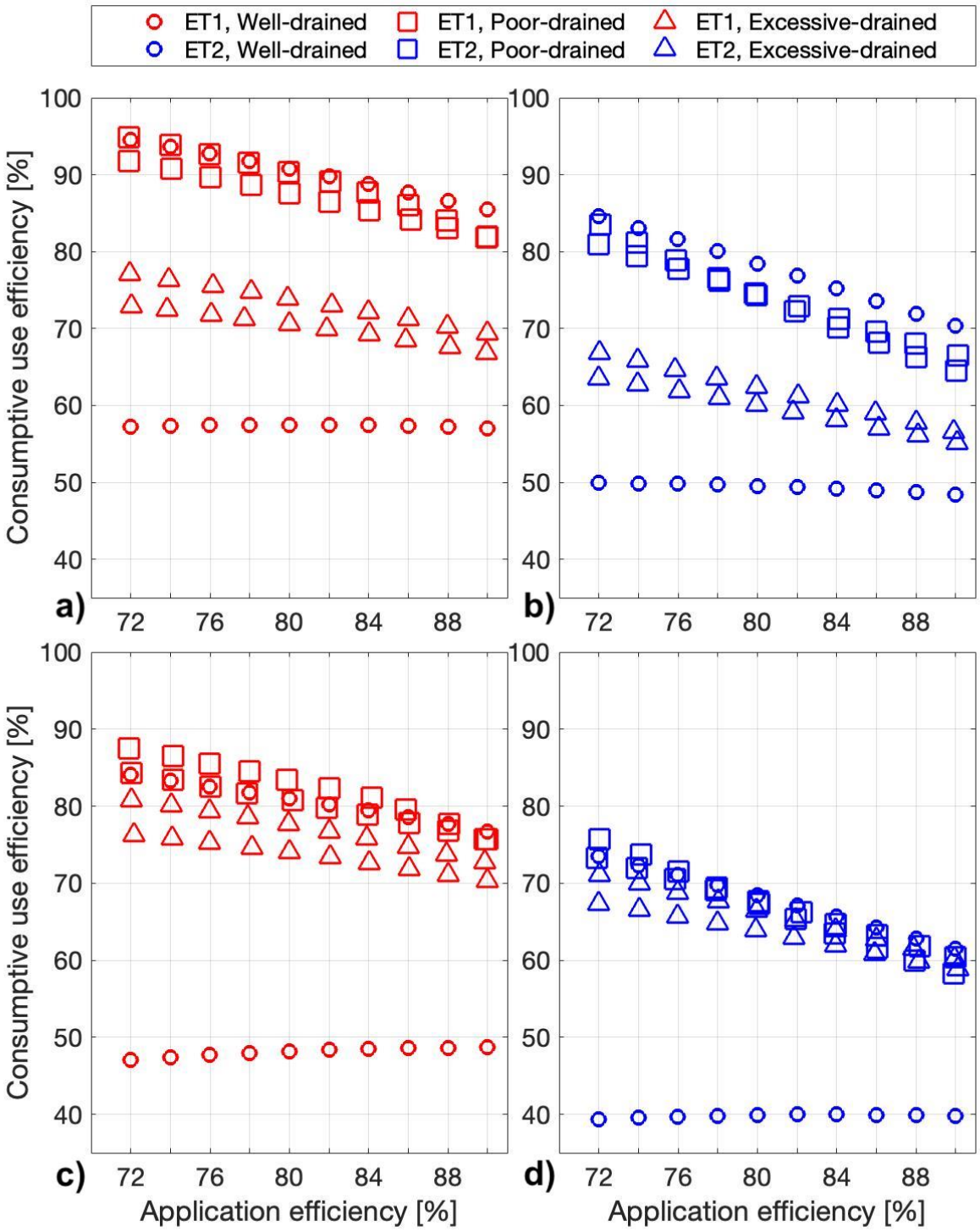

Figure 3.5 Consumptive Use Efficiency for Test Scenarios. For graphs a) and b), initial SWC was set at FC or "wet" conditions. Graphs c) and d) describe "dry" conditions where initial SWC was set at MAD. Test scenarios using a one-day irrigation schedule are shown. Only model runs testing the upper and lower drainage rate values are shown.

The most prevalent relationship for these test scenarios was a decreasing trend of CUE with increasing application efficiency. In other words, as more effective irrigation is applied to the crop, deep infiltration increases. Adjusting the *b* parameter, which essentially represents the rate of soil drainage, had a noticeable effect on CUE. Faster drainage rates are shown in Figure 3.5 with lower CUE, where slower rates are shown with comparatively higher CUE. As the *b* parameter approaches zero and the rate of drainage slows, CUE decreases with increasing AE. As the *b* parameter becomes more negative and drainage rates increase, CUE (and deep infiltration) show less variation.

These relationships suggest both the rate of soil drainage and the application efficiency of the irrigation system have influence on deep infiltration. AE has a stronger negative relationship on CUE when the rate of drainage is slower (i.e., *b* parameter approaches zero). Slower drainage rates allow the roots to extract more water used towards ET. Increased depths of effective irrigation must match the rate of root water extraction (RWE) while also not exceeding the water holding capacity of the root zone. These relationships also suggest how irrigation scheduling can improve the consumptive use efficiency of applied water. When irrigation schedules consider climatic factors, such as the atmospheric demand for water (ET), deep infiltration losses can decrease by about 10% (Figure 3.5).

Ideally, irrigation systems with increased AE should improve the CUE of applied irrigation. This relationship is slightly evident in Figure 3.5, graph c). This test scenario demonstrates a “dry” winter followed by a “dry” summer; in other words, winter precipitation was low and growing season atmospheric conditions were warm. In such situations, the irrigator will likely need to apply greater depths of irrigation to replenish soil water storage and keep up with the crop water requirement. It happens that the irrigation prescription for this test scenario was able to apply water more efficiency with increasing AE. Since this relationship only improves CUE by less than one percent and it is only evident for a few test scenarios, further research will be required to understand the underlying effects. Still, it is hypothesized that irrigation management that use “best management practices” (BMPs) when prescribing irrigation can improve CUE with improved irrigation systems. BMPs could include keeping a record of soil moisture content or utilizing weather-based ET estimates. This has been echoed by the Congressional Research Service in addressing government

subsidies provided to agricultural producers for adoption of irrigation technologies (Stubbs, 2016).

Estimated Total Seasonal Yield Reduction

Irrigators water crops for the main purpose of maximizing crop yield through supplementing water lost to ET. When it comes to water conservation at the farm scale, one incentive for irrigators to adopt irrigation technologies with higher AE is to reduce power costs. Water pumped to the field and driven by center pivot systems uses a substantial amount of power in the irrigation process. From an economic perspective of the irrigator, investment in irrigation technologies will have to be met by financial savings in power consumption, as well as continued or improved crop yields. The question lies from these modeled scenarios is whether crop yields can be maintained with decreased deep infiltration losses. To do so, a seasonal yield reduction (YR_{seas}) metric was used to estimate yield loss experienced by a plant due to water stress. Within the DI model, each layer of the soil profile assigns a water stress factor (Ks) based on total soil water potential (Eq. 2.3). When Ks < 1 water stress occurs, and plant transpiration and growth are hindered. Yield loss has been described for many crops using first-order approximations, a relationship that appears to be consistent against cultivars of alfalfa (Steduto et al., 2012). YR_{seas} is estimated in this study using a similar approach as the Irrigation Scheduler tool by Peters et al. (2019), where yield reduction is a function of the water stress factor:

$$YR_{seas} = 1 - \left(\frac{\sum_{i=1}^{192} (Ks_{LYR1(i)} + Ks_{LYR2(i)} + Ks_{LYR3(i)})}{192} \right) \cdot 100 \qquad \text{(Eq. 3.4)}$$

Where YR_{seas} is the total seasonal yield reduction [%], Ks is the stress coefficient [fraction] for each given layer, and 192 is the number of modeled days for each test scenario. This equation assumes that water stress had a negative linear correlation with crop yield, and YR_{seas} can be estimated using the season-long average Ks.

Figure 3.6 shows application efficiency versus estimated total seasonal yield reduction for test scenarios. As before, a one-day irrigation schedule and the upper and lower ranges for *b* parameter values are shown in the graphs. The most evident relationship is that as AE increases, the average seasonal yield reduction decreases. As more water is applied to the soil

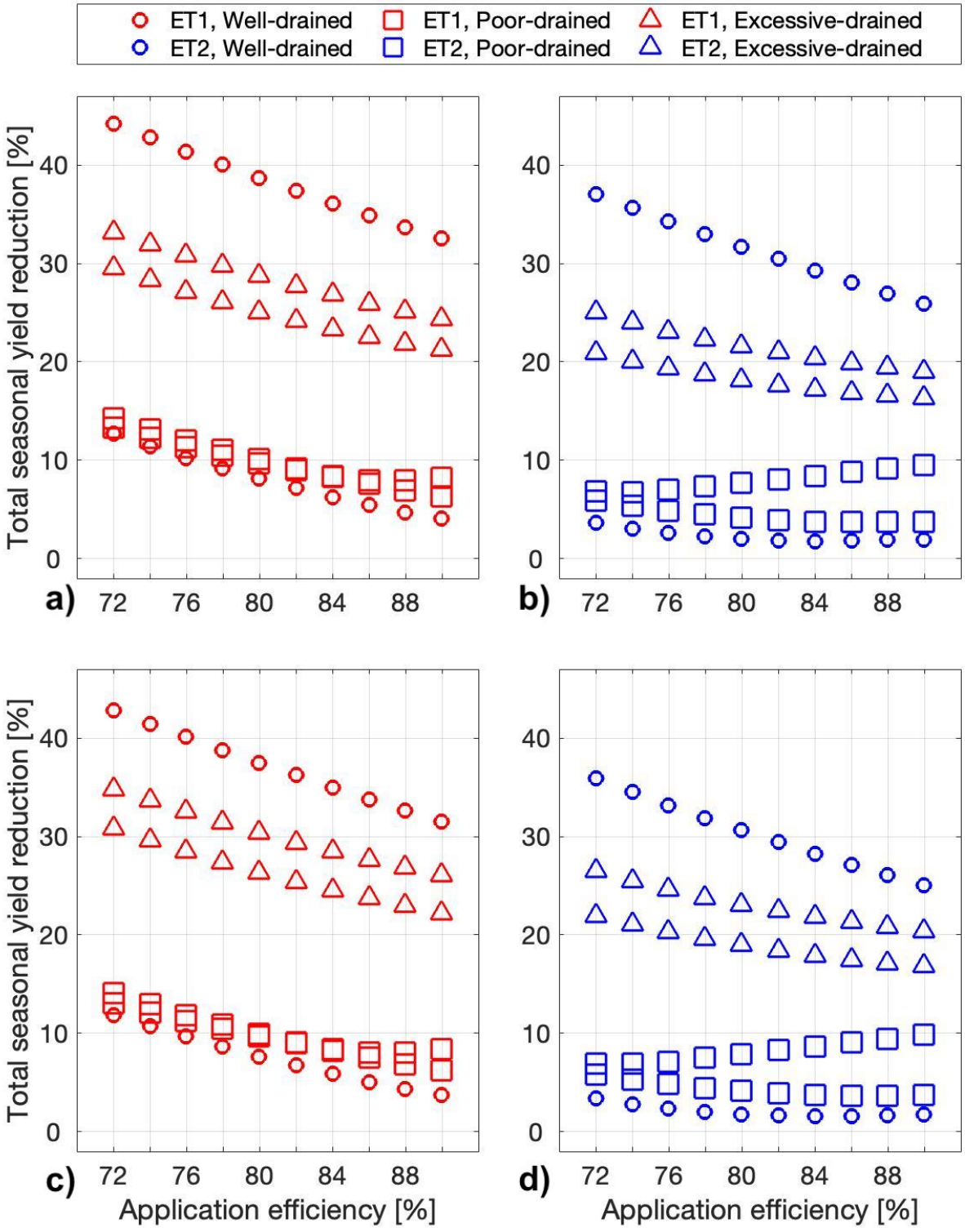

Figure 3.6 Seasonal Yield Reduction for Test Scenarios. For graphs a) and b), initial SWC was set at FC or "wet" conditions. Graphs c) and d) describe "dry" conditions where initial SWC was set at MAD. Test scenarios using a one-day irrigation schedule are shown. Only model runs testing the upper and lower drainage rate values are shown.

surface due to increased application efficiency, there is decreased likelihood the crop will experience water stress. This relationship is largely intuitive, though it does not hold true for some test scenarios for excessive-drained soils. The pattern breaks for excessive-drained soils that were tested with the upper range of *b* parameter values (-0.27). As the *b* parameter approaches zero the soil drainage rate can be described as "slow". Figure 3.7 shows one model run that resulted in increased YR_{seas} with higher application efficiency. For layer 1 (Figure 3.7, graph a), saturated water stress was consistent throughout the season, as designated by red triangle markers. Whether this is a realistic situation for "excessive-drained" soils requires further analysis of the soils data and *b* parameter ranges. This situation highlights one aspect of the model that could use further research.

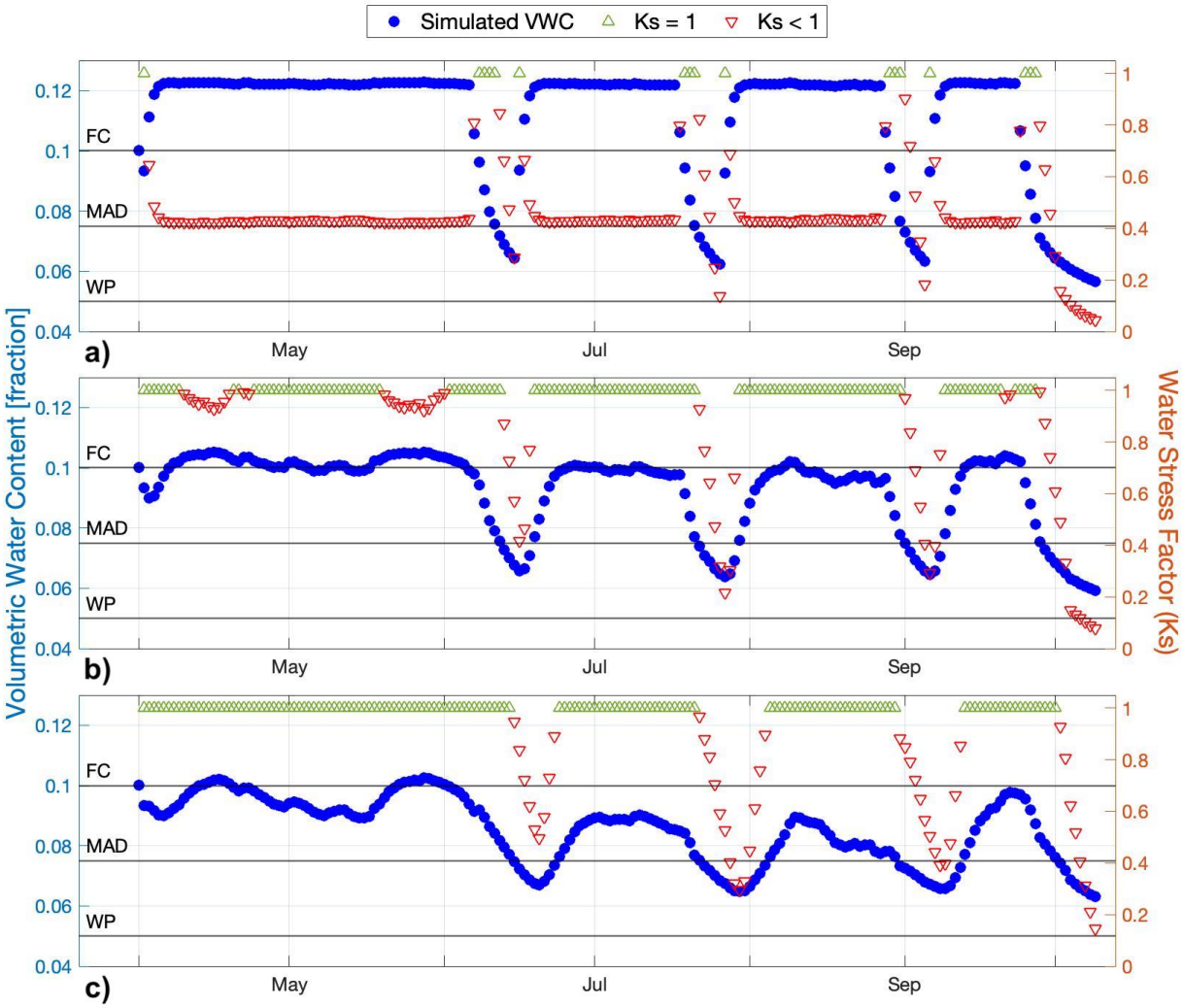

Figure 3.7 Excessive-Drained Soils with High AE. This figure is used to show saturated water stress in layer 1 (graph a) that resulted due to increased AE and slow drainage rates given by parameter *b*. Green markers denote soil water conditions that are stress-free, or Ks = 1. AE was set at 90% for this model run.

From a management perspective, irrigators would likely avoid conditions that lead to over-saturation of the surface soil layer. This leads to challenges for center pivot systems, as motor wheels can become stuck with too much applied irrigation. From a modelling perspective, surface ponding can contribute to surface runoff, which is water balance term not accounted for. Additionally, the model does not account for surface runoff or evaporation from pooling, which could occur when layer 1 exceeds field capacity. The model run from Figure 3.7 also highlights a challenge of the Magic Valley DI study, which required estimating drainage parameters for three dominant soil drainage classes. Further development of the model could utilize in-situ soil data for excessive-drained soils to validate simulated SWC for layer 1.

The deep infiltration results for the Magic Valley study were presented in this section in terms of consumptive use efficiency. CUE was used primarily to compare model results with a related metric of application efficiency. The results of this study could be used to guide decisions for regional water balance estimates. Since growing conditions were generalized for the entire Magic Valley region, there is uncertainty for all model parameters and absolute values for DI are not shown explicitly. As a baseline comparison of absolute DI found from the Magic Valley study, Table 3.4 shows cumulative seasonal DI resulting from calibration and validation model runs presented in Chapter 2. These model runs used observed SWC and actual ET data from Harney Basin to simulate deep infiltration for alfalfa.

Table 3.4 Comparison of Absolute DI Estimates for Magic Valley.

Model Run	Soil Drainage Type	Deep Infiltration Range [mm]
Magic Valley DI Study	Well-drained	45 – 554
Magic Valley DI Study	Poor-drained	41 – 264
Magic Valley DI Study	Excessive-drained	164 – 355
DI Model Calibration (2018)	Well-drained	115 – 136
DI Model Validation (2019)	Well-drained	97 – 120
DI Model Validation (2020)	Well-drained	259 – 261

Chapter 4: Considerations of Agricultural Water Balance Estimates for Regional Water Management

Irrigation is the largest user of freshwater resources, and likely the most important in meeting the world's food supply. Irrigated agriculture represents 70 percent of global water withdrawals, the largest water footprint compared to other sectors (Siebert et al., 2010). Demand for agricultural products is high and projected to continue supporting a growing population and biofuel industry. This puts pressure on irrigated agriculture which already faces large uncertainties due to climate change, such as "extreme" weather conditions and interannual variability in water supply. Water security is needed to ensure food security, which has been said to be the greatest challenge of our century (Easterling, 2007).

The sustainability of irrigated agriculture requires accounting for irrigation's part in regional water balances. Irrigation is unique from other water users since a large portion of water is removed from supply without return to the hydrologic system; in other words, irrigation has a high "consumptive use" or ET requirement. Crop consumptive use was estimated as 62 percent of withdrawals for the US in 2015 (Dieter et al., 2018). Additionally, irrigation consumes both surface and groundwater sources. In the past 50 years, groundwater withdrawals have tripled (World Water Assessment Programme, 2012). While this has expanded the acreage of arable lands, it has also led to declining aquifer levels worldwide as withdrawals exceed the rate of natural recharge.

Due to irrigation's significant impact on water supply, policy and management decisions of the past couple decades have focused on water "savings" within the agricultural sector. Federal policies have subsidized irrigation technology with the goal of increasing water use efficiency. The paradox of improved irrigation efficiency is that in many cases, it has led to increased water consumption per acre (Grafton et al., 2018; Perry and Steduto, 2017; Ward and Pulido-Velazquez, 2008). In addition, adoption of irrigation technologies has decreased the amount of incidental aquifer recharge. This was true for the Eastern Snake Plain Aquifer in southeast Idaho, which saw an increase in improved irrigation in the 1950s. Coupled with canal lining and a decline in farmers using traditional flood irrigation, the aquifer saw a steady decline in aquifer storage of about 200,000 acre-feet-year (Stewart-Maddox et al., 2018).

Considering the paradoxes related to improved irrigation efficiency, the DI model was developed to provide another tool by which agricultural water resources can be quantified. The DI model was applied to irrigated alfalfa in the Magic Valley region, in which deep infiltration was evaluated in context of improved "application efficiency" (AE). AE describes the amount of water applied to the root zone over the amount of water delivered to the farm via a conveyance system (Irmak et al., 2011). This metric largely describes inefficiencies related to wind drift or evaporation from the canopy. The model estimated "soil water storage efficiency" that resulted from increased AE cited for modified irrigation systems. Soil water storage efficiency describes the volume of water stored in the root zone of a crop over the volume that exceeds the root zone water holding capacity and is lost to deep infiltration (Irmak et al., 2011). As opposed to the application efficiency, which describes losses from applied irrigation to surface processes like wind and evaporation, soil water storage efficiency emphasizes subsurface losses from irrigation. It was found from the regional DI study in Chapter 3 that increasing the AE for irrigation systems will decrease the soil water storage efficiency by as much as 60 percent. Modified irrigation systems that have higher AE include Low Elevation Spray Application (LESA) and Low Energy Precision Application (LEPA). These irrigation designs apply water at lower pressure in closer proximity to the soil surface. It was found that as AE increased, so did the amount of irrigation add to the root zone.

The test results from the DI model not only illustrate the model's applicability for farm-scale management and irrigation scheduling, but also provides an engineering-based tool to account for soil water infiltration from near-surface processes. Estimating losses from deep infiltration from irrigated agriculture could be used in larger modeling applications related to aquifer recharge. This chapter discusses the wider relevance of the DI model in context of conjunctive management and administration of water rights in southeast Idaho. A regional hydrologic model is used to estimate recharge and spring discharge from the Eastern Snake Plain Aquifer (ESPA). This model is used as an "administrative factfinding" tool to support the conjunctive administration of surface water and groundwater rights in the region (Tuthill et al., 2013).

History of Aquifer

The Eastern Snake Plain Aquifer is located in the southeast corner of Idaho and is one of the world's most productive aquifers. This aquifer is key in supporting the state's agricultural industry, which provides about half of the water for 2.1 million irrigated acres of farmland on the ESPA (Stewart-Maddox et al., 2018). Initially, irrigation in southern Idaho was isolated to surface water diversions and canal systems. Around the 1950's, groundwater withdrawals increased significantly, as did the number of arable lands across the Eastern Snake Plain (ESP). This period also saw adoption of sprinkler irrigation technology, which increased the application efficiency of irrigation compared to flood methods. Improved irrigation efficiencies decreased the amount of "incidental recharge", a term that describes infiltration from human activities to groundwater. Due to these factors, aquifer levels began to steadily decline and create water shortages for surface water right holders. It became evident the Eastern Snake Plain is a highly connected hydrologic system; surface water and groundwater are intricately linked. Southern Idaho geology is primarily fractured basalt. The collective thickness of basalt flows in the ESP exceed thousands of feet (Cosgrove et al., 1999). Extensive, well-fractured geology transmits water easily and creates highly responsive aquifers.

Regional Groundwater Modeling using ESPAM

To support water resource management and conjunctive administration in Idaho, a groundwater model for the ESPA was first initiated by Idaho Department of Water Resources (IDWR). The model serves as the "factfinding" or scientific tool by which justification of state policy decisions can be made. Water management decisions such as curtailment of junior water rights are supported with data from the model (Tuthill et al., 2013). The currently used model is the Enhanced Snake Plain Aquifer Model (ESPAM) (Hoekema and Sridhar, 2013). The model is supported by an inter-agency collaboration of hydrologists, modelers, private industry members, and the University of Idaho (*idwr.idaho.gov/water-data/projects/ESPAM/, Accessed October 2021)*. Model developments are focused on interactions between the aquifer and the Snake River, as well spring discharges in proximity to the aquifer (IDWR, 2013).

Given the applicability of irrigated-induced recharge to aquifer modeling, the

DI model is considered in context of ESPAM. ESPAM is a temporally and spatially explicit model. Recharge, a net increase in aquifer storage, is the major model output and is calculated for one-month periods for separate surface water entities within the ESPA boundaries. Net recharge from "surface-water irrigated lands" is estimated using a water balance approach (IDWR, 2013). Surface-water irrigation describes the source type (i.e., not groundwater), as estimates for on-farm water delivery are taken from diversion records. Deep infiltration (ft/month) from surface-irrigated lands is calculated with an algorithm that considers on-farm water balance components. This algorithm is a simple algebraic equation that includes effective precipitation, "maximum on-farm efficiency", headgate delivery to farm, an ET adjustment factor, change in soil moisture, and an "initial loss" and "excess delivery" factor for deep infiltration (IDWR, 2013). The maximum on-farm efficiency is set to 0.85 for sprinkler and 0.80 for flood irrigation. This efficiency term in not the same as application efficiency, but a corrective factor that adjusts the amount of water delivered to farm during water shortages. The "initial loss" and "excess delivery" factors for DI are more similar to AE in which they describe the amount of water not consumed directly through ET. The "initial loss" is the fraction of surface runoff that goes towards DI, where "excess delivery" is the fraction of DI due to excess application in meeting the crop water requirement.

From ESPAM simulations between 1980 and 2008, it was found there was about 1.9 million acre-feet variation in net recharge from surface-water irrigation, which is attributed to changes in water supply and the role of irrigation in aquifer recharge (IDWR, 2013). Total cumulative change in aquifer storage for 1980-2008 showed a decrease in 6.2 million acre-feet (Patton, 2011). Based on these cited values, irrigation-induced recharge accounted for about 30 percent of total aquifer storage change. For ESPAM simulations ran for recent water years, the irrigation efficiencies are largely an estimated value based on irrigation "entities". In this context, the DI model can be applied over an irrigation entity as way to estimate DI for variable irrigation management strategies. With more fields in the ESP converting to sprinkler application, incidental recharge to the aquifer will likely decrease with fewer flood irrigated fields. If the ESP shows increased adoption of pressurized irrigation, it might be useful to account for different types of sprinkler systems. For example, a high impact sprinkler system has shown application efficiencies (AE) between 50-60

percent, where center-pivot system AE are estimated at 70-85 percent (Sterling and Neibling, 1994). The DI model has shown higher AE systems can lead to increased DI. Inefficiencies related to DI can increase by as much as 10 percent given the atmospheric conditions governing ET.

Another advantage of the DI model is it simulates soil water content on a daily time step. Changes in soil water content are calculated monthly in ESPAM. Variations in the crop water requirement (ET) are accounted for on a shorter time scale in the DI model, which can improve estimates in water balance components used in the ESPAM. Temporal changes in deep infiltration could be significant if irrigators practice deficit irrigation in water short years. This is relevant to alfalfa production in the Magic Valley, where this forage type is known for its resiliency to water stress. Modeling efforts specific to crop type and irrigation management decisions could play a significant role in future years within the ESPA. Overall, the DI model is an applied tool by which near-surface boundary conditions estimates of DI can be used to support regional water balances.

Conjunctive Administration in the Eastern Snake Plain

Groundwater resources from the ESPA are used for irrigation, hydropower, trout production, domestic, municipal, and industrial water uses. With decreasing trends in aquifer storage, resource conflict between water rights holders have escalated. Surface water users were impaired by groundwater users due to decreased spring discharges from the aquifer. To mitigate these issues, “delivery calls” could be made to the state regulatory agency (IDWR). Delivery calls were made by senior water right holders who hold “first in priority” status to water use. “Priority” refers to the Western water law of “Prior Appropriation”, which allows earlier established water rights to use water first in times of shortage. For senior holder’s water right to be satisfied, these delivery calls sometimes curtailed or amended a junior water right’s allocation, who follow second in priority to senior users. These procedures evolved from the passing of the 1951 Idaho Ground Water Act, which provided a foundation for the “conjunctive administration” of surface and groundwater rights. In 2005, the handling of delivery calls was refined, where the court emphasized the need for IDWR to provide “administrative factfinding” to show the impact of groundwater use on surface water (or vice versa), as well as evaluating the storage of the surface water right user before

curtailing or amending the junior groundwater right (Tuthill et al., 2013). The ESPAM was used to meet the needs for improved water accounting of surface and groundwater rights.

Where the ESPAM model has a main goal of optimizing surface water and groundwater resources within southeast Idaho, the term "conjunctive administration" refers to the State's regulatory power to administer groundwater and surface water rights in the Eastern Snake Plain based on priority. With factual support from the state agency (IDWR), an order can be made to curtail water from a junior holder. IDWR and its director hold the legal authorization to control water within distribution entities, such as state water districts. The director works with watermasters in allocations, especially in times of shortage. Around 2003, the director authorized watermasters to also administer groundwater rights in addition to surface water sources (Tuthill et al, 2013). This new provision allows water districts to develop mitigation plans in times of drought and help maintain aquifer storage for future use.

Conjunctive administration has regularly dealt with conflict between surface water and groundwater irrigators, largely due to reduced spring river flows from aquifer storage decline. Recently, irrigators in the ESP took part in a historic mitigation plan to reduce conflict and work towards restoring aquifer levels to previous conditions in the 1990's. The mitigation plan is outlined in the 2015 Settlement Agreement, in which seven canal companies, called collectively the Surface Water Coalition (SWC), and ten groundwater districts, represented by Idaho Ground Water Appropriators, Inc. (IGWA) took part in. Leading up to the agreement in 2015, several water calls were made that could potentially curtail junior users throughout the ESP. These junior users not only include groundwater irrigators, but also industrial and municipal entities that use groundwater.

It was decided an agreement between willing parties would be a more proactive solution than fighting over rights in court. The agreement outlines a plan to work towards stable aquifer levels, with IGWA recharging 110,000 acre-feet with total groundwater diversion reduced by 240,000 acre-feet annually (Olson et al., 2016). Additionally, the settlement objectives were to mitigate further injury to the senior right holders and minimize economic impact due to water shortages (Olson et al., 2016). In 2016, with the settlement already in effect, a curtailment order was released by the Director of IDWR to account for a predicted shortfall in the groundwater supply. Junior water rights holders not affiliated with

the 2015 Settlement faced curtailment, while others under the settlement were required to cut down groundwater withdrawals from between 4-20 percent (Running et al., 2019). Thus, irrigators were required to adapt to changes in water availability in order to reduce economic loss.

Running et al. identified adaption practices taken by Idaho farmers in response to 2015 Settlement restrictions on groundwater pumping (2019). Based on 265 respondents, the two most commonly adopted practices to reduce groundwater pumping were improvements to irrigation system efficiency (77%) and reduction in spending (67%) (Running et al., 2019). Other adaptive strategies include irrigating less frequently or changing crop rotation. Findings from this survey show irrigation efficiency is a widely adopted practice to reduce groundwater pumping. A question that arises from these findings is, did groundwater pumping truly decrease with adoption of more efficient irrigation systems?

One way to address this question is by analyzing consumptive use estimates for the areas that faced groundwater reductions. With less pumping, it is assumed less water is being applied to support crop evapotranspiration. Actual ET (ET_a) maps provided by IDWR were used to quantify consumptive use for years proceeding and following the 2015 Settlement Agreement. These maps are made using Landsat satellite images, which are later used in the METRIC model (Mapping EvapoTranspiration at high Resolution with Internalized Calibration). This model calculates actual ET as the residual of a surface energy balance. Total seasonal ET_a was tabulated for years 2009-2018 for groundwater districts within the Eastern Snake Plain. A seven-year average period (2009-2015, excluding 2012 and 2014) was used to compare with ET_a in years following the 2015 agreement. An annual difference of years 2016, 2017 and 2018 were taken from the seven-year averaging period. The results show consumptive use was statistically reduced for all groundwater districts following the agreement. Another question lies that if groundwater pumping was reduced to show a decrease in ET, were farmers able to support the same crop yields as before the settlement? If so, this implies adaptive strategies, like adopting efficient irrigation systems, are able to use “more crop per drop.” Future studies related to water productivity in the ESPA could compliment these findings and answer questions about the efficacy of irrigation technologies.

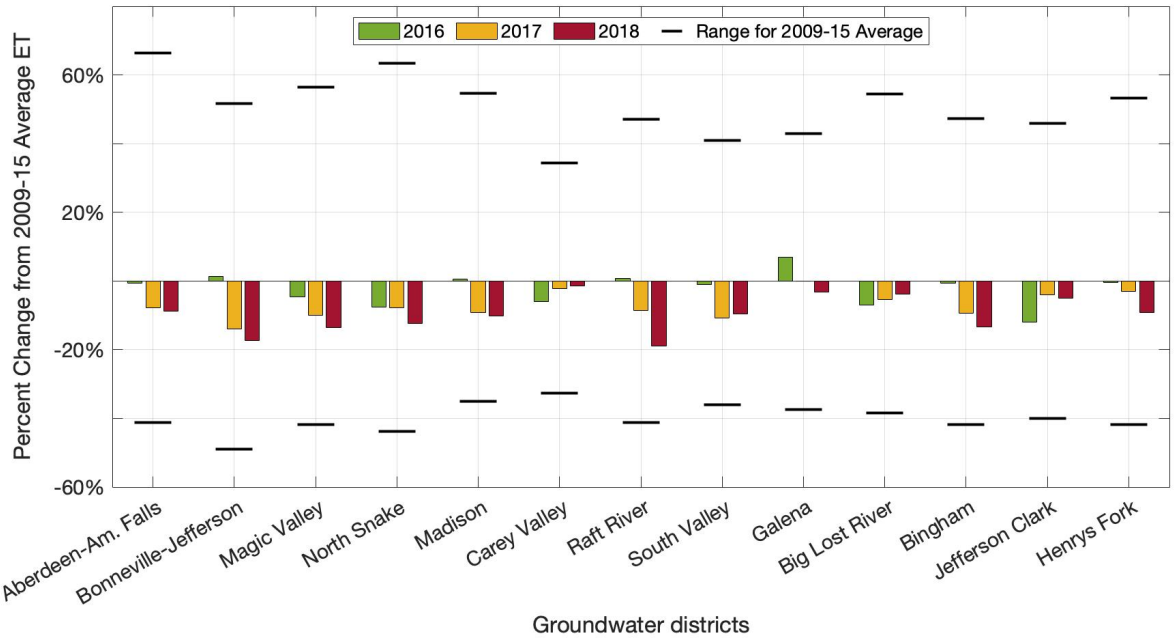

Figure 4.1 Consumptive Use Study for ESPA Groundwater Districts. Total seasonal ETa for years 2009-2015 were used to provide an average of preceding growing conditions before the 2015 Settlement Agreement. Groundwater districts shown are those that overly the ESPA.

The 2015 Settlement Agreement imposed challenges for many junior rights holders who were asked to curtail their groundwater pumping. With droughts following the settlement, junior holders were faced with both physical shortages and allocation cutbacks. Adoptive strategies were necessary for irrigators to support crop production and will likely continue to play a role for future projections of water scarcity. In a semi-arid environment, like southeast Idaho, water management and policy focus on maintaining aquifer storage. The aquifer acts as an underground reservoir that can be relied on regardless of interannual surface water supply. Water accounting tools that help monitor aquifer recharge will be needed for supporting the economic sustainability of irrigated agriculture in Idaho.

Conclusion

Water shortages of today, and uncertainties about water supply in the future, highlight the need for water resource accounting. Scientifically grounded methods in water accounting help inform water policy decisions and the administration of water rights in areas

with limited resources. For areas that rely on irrigation to support agricultural productivity, water shortages can impact regional economy and create conflict between water users. Adaptive solutions to water shortages focus on the irrigation sector, which account for 70 percent of freshwater withdrawals worldwide. Water savings from irrigated agriculture are expected to alleviate total water abstractions from hydrologic systems.

One method for conserving water resources in agriculture is through adoption of irrigation technologies. These technologies primarily focus on reducing water losses that occur between water delivery to the field and application to the crop surface. The paradox of irrigation efficiency is it does not always lead to water savings. Irrigation efficiency has been shown to increase the amount of irrigated land, as well as indirectly reduce water availability to downstream users. It is suggested that a better description and accounting of the physical principles underlying "irrigation efficiency" be undertaken to truly promote water savings (Willardson et al., 1994; Grafton et al., 2018). This study evaluated irrigation efficiency by developing a model by which deep infiltration from irrigated agriculture can be quantified. The DI model simulates water content for a defined root zone, which is used to estimate near-surface DI resulting from irrigation events. Soil water storage efficiency was calculated as the ratio of water used directly for crop growth over the amount of effective irrigation applied to the crop surface. After testing the DI model over a range of climatic conditions and management types for the Magic Valley region, it was found soil water storage efficiency decreases with increased application efficiency (AE). This knowledge becomes useful when promoting irrigation technology for on-farm and regional water savings. These technologies do have potential for water savings, as Figure 4.1 suggests through reduction of consumptive use. These technologies are likely to succeed in overall irrigation efficiency when coupled with best management practices (BMPs). The Magic Valley DI study emphasized that a one-fits-all irrigation prescription for pressurized irrigation systems will lead to deep infiltration losses. Accounting for the crop water requirement, soil texture and drainage rate, as well as precedent soil moisture conditions can increase water use efficiency by 10 percent (Chapter 3, Figure 3.5).

Irrigation efficiency is a variable within regional groundwater models, like ESPAM. Applied tools such as the Deep Infiltration Model can help support regional water balance models by providing a baseline estimate of DI, and more specifically evaluate losses to deep

infiltration due to irrigation technology. DI estimates have relevance for watersheds that conjunctively manage surface water and groundwater rights. It is predicted that semi-arid regions will need to rely on aquifer storage to offset interannual variability in water supply due to climate change. Estimates of near-surface DI from irrigated agriculture can support a holistic approach in water resource accounting.

Bibliography

Adler, Jonathan H. (2009). Warming Up to Water Markets. Regulation, Vol. 31, No. 4, Winter 2008-2009, Case Legal Studies Research Paper No. 09-4, Available at SSRN: https://ssrn.com/abstract=1341061

Allen, R.G. (2006). Footprint Analysis to Assess the Conditioning of Temperature and Humidity Measurements in a Weather Station Vicinity. *World Environmental and Water Resource Congress 2006*, 1–12. https://doi.org/10.1061/40856(200)292

Allen, R.G., Burnett, B., Kramber, W., Huntington, J., Kjaersgaard, J., Kilic, A., Kelly, C., & Trezza, R. (2013). Automated Calibration of the METRIC-Landsat Evapotranspiration Process. *JAWRA Journal of the American Water Resources Association*, *49*(3), 563–576. https://doi.org/10.1111/jawr.12056

Allen, R.G., Irmak, A., Trezza, R., Hendrickx, J.M.H., Bastiaanssen, W., & Kjaersgaard, J. (2011). Satellite-based ET estimation in agriculture using SEBAL and METRIC. Hydrol. Process., 17.

Allen, R. G., Pereira, L. S., Howell, T. A., & Jensen, M. E. (2011). Evapotranspiration information reporting: I. Factors governing measurement accuracy. *Agricultural Water Management*, *98*(6), 899– 920. https://doi.org/10.1016/j.agwat.2010.12.015

Allen, R., Pereira, L., Raes, D., & Smith, M. (1998). Crop Evapotranspiration: Guidelines for computing crop water requirements. FAO (Food and Agriculture Organization) Irrigation and drainage paper No. 56. *Rome: Food and Agriculture Organization of the United Nations*, *56*, 26–40.

Allen, R.G., Pereira, L.S., Smith, M., Raes, D., & Wright, J.L. (2005). FAO-56 Dual Crop Coefficient Method for Estimating Evaporation from Soil and Application Extensions. *Journal of Irrigation and Drainage Engineering*, *131*(1), 2–13. https://doi.org/10.1061/(ASCE)0733-9437(2005)131:1(2)

Allen, R. G., Tasumi, M., & Trezza, R. (2007). Satellite-Based Energy Balance for Mapping Evapotranspiration with Internalized Calibration (METRIC)—Model. *Journal of Irrigation and Drainage Engineering*, *133*(4), 380–394. https://doi.org/10.1061/(ASCE)0733-9437(2007)133:4(380)

Arnold, J.G., Moriasi, D.N., Gassman, P.W., Abbaspour, K.C., White, M.J., Srinivasan, R., Santhi, C., Harmel, R.D., Griensven, A. van, Liew, M.W., Kannan, N., & Jha, M.K. (2012). SWAT: Model Use, Calibration, and Validation. *Transactions of the ASABE*, *55*(4), 1491–1508. https://doi.org/10.13031/2013.42256

ASCE-EWRI. (2005). *The ASCE standardized reference evapotranspiration equation.* ASCE-EWRI Standardization of Reference Evapotranspiration Task Comm. Report, ASCE Bookstore, ISBN: 078440805, Stock Number 40805; 216.

Bastiaanssen, W. G. M., Noordman, E. J. M., Pelgrum, H., Davids, G., Thoreson, B. P., & Allen, R. G. (2005). SEBAL Model with Remotely Sensed Data to Improve Water-Resources Management under Actual Field Conditions. *Journal of Irrigation and Drainage Engineering*, *131*(1), 85–93. https://doi.org/10.1061/(ASCE)0733-9437(2005)131:1(85)

Bauder, J.W. (1978). *Irrigating alfalfa: Some guidelines. Washington State University*. https://waterquality.montana.edu/farm-ranch/irrigation/alfalfa/guidelines.html

Bethune, M.G., Selle, B., & Wang, Q.J. (2008). Understanding and predicting deep percolation under surface irrigation. *Water Resources Research*, *44*(12). https://doi.org/10.1029 ~/2007WR006380

Bowen, J.S. (1926). The ratio of heat losses by conduction and by evaporation from any water surface. Phys Rev 27:779–787

Cai, X., & Rosegrant, M. W. (2002). Global Water Demand and Supply Projections: Part 1. A Modeling Approach. *Water International*, *27*(2), 159–169. https://doi.org/10.1080/02508060208686989

Campbell Scientific, Inc. (2008). *EdiRe Software for Micrometeorological Applications*. Campbell Scientific, Inc.

Campbell Scientific, Inc. (2020). *CS616 and CS625: Water Content Reflectometers.* Manual. https://s.campbellsci.com/documents/us/manuals/cs616.pdf

Colaizzi, P., Gowda, P., Marek, T., & Porter, D. (2009). Irrigation in the Texas High Plains: A Brief History and Potential Reductions in Demand. *Irrigation and Drainage*, *58*, 257–274. https://doi.org/10.1002/ird.418

Cosgrove, M. J., Wilson, J., Watt, D., & Grant, S. F. (1999). The relationship between selected physiological variables of rowers and rowing performance as determined by a 2000 m ergometer test. *Journal of Sports Sciences*, *17*(11), 845–852. https://doi.org/10.1080/026404199365407

Dieter, C.A., Maupin, M.A., Caldwell, R.R., Harris, M.A., Ivahnenko, T.I., Lovelace, J.K., Barber, N.L., & Linsey, K.S. (2018). *Estimated use of water in the United States in 2015* (Report No. 1441; Circular, p. 76). USGS Publications Warehouse. https://doi.org/10.3133/cir1441

Easterling, W. E. (2007). Climate change and the adequacy of food and timber in the 21st century. *Proceedings of the National Academy of Sciences*, *104*(50), 19679–19679. https://doi.org/10.1073/pnas.0710388104

Ellis, S. (2019). Dairy a major part of Idaho's economy. *Idaho Farm Bureau Federation*. https://www.idahofb.org/News-Media/2019/11/dairy-a-major-part-of

Ellis, S. (2021). Report: Ag has massive impact on Magic Valley economy. *Idaho Farm Bureau Federation.* https://www.idahofb.org/News-Media/2021/03/report-ag-has-massive-impact

Ershadi, A., McCabe, M. F., Evans, J. P., & Walker, J. P. (2013). Effects of spatial aggregation on the multi-scale estimation of evapotranspiration. *Remote Sensing of Environment*, *131*, 51–62. https://doi.org/10.1016/j.rse.2012.12.007

Esri Inc. (2021). *ArcGIS Desktop* (Version 10.5). Esri Inc. https://www.esri.com/en-us/arcgis/products/arcgis-desktop/overview

Farahani, H. J., Howell, T. A., Shuttleworth, W. J., & Bausch, W. C. (2007). Evapotranspiration: Progress in Measurement and Modeling in Agriculture. Transactions of the ASABE, 50(5), 1627–1638. https://doi.org/10.13031/2013.2396

Gassman, P.W., Williams, J.R., Benson, V. W., Izaurralde, R.C., Hauck, Jones, C.A., Atwood, J.D., Kiniry, J.R., & Flowers, J.D. (2004). Historical Development and Applications of the EPIC and APEX models. *2004, Ottawa, Canada August 1 - 4, 2004*. 2004, Ottawa, Canada August 1 - 4, 2004. https://doi.org/10.13031/2013.17074

Grafton, R., Williams, J., Perry, C. J., Molle, F., Ringler, C., Steduto, P., Udall, B., Wheeler, S., Wang, Y., Garrick, D., & Allen, R. (2018). The paradox of irrigation efficiency. *Science*, *361*, 748–750. https://doi.org/10.1126/science.aat9314

Grantham, T.E., & Viers, J.H. (2014). 100 years of California's water rights system: Patterns, trends and uncertainty. *Environmental Research Letters*, *9*(8), 084012. https://doi.org/10.1088 ~/1748-9326/9/8/084012

Gowda, P.H., Howell, T.A., Chávez, J.L., Paul, G., Moorhead, J.E., Holman, D., Marek, T.H., Porter, D., Colaizzi, P.D., Evett, S.R., & Brauer, D.K. (2015). A Decade of Remote Sensing and Evapotranspiration Research at USDA-ARS Conservation and Production Research Laboratory. *2015 ASABE / IA Irrigation Symposium: Emerging Technologies for Sustainable Irrigation - A Tribute to the Career of Terry Howell, Sr. Conference Proceedings*, 1–14. https://doi.org~ /10.13031/irrig.20152143458

Ha, W., Gowda, P. H., & Howell, T. A. (2013). A review of downscaling methods for remote sensing- based irrigation management: Part I. *Irrigation Science*, *31*(4), 831–850. https://doi.org/10.1007/s00271-012-0331-7

Hatiye, S., Prasad, K., Ojha, C., & Adeloye, A. (2016). Estimation and Characterization of Deep Percolation from Rice and Berseem Fields Using Lysimeter Experiments on Sandy Loam Soil. *Journal of Hydrologic Engineering*, *21*, 05016006. https://doi.org/10.1061/(ASCE)HE.1943-5584.0001365

Hines, S., & Neibling, H. (2013). *Center Pivot Irrigation for Corn: Water Management and System Design Considerations in Southern Idaho*. 12.

Hoekema, David J. and Sridhar, Venkataramana. (2013). A System Dynamics Model for Conjunctive Management of Water Resources in the Snake River Basin. *Journal of the American Water Resources Association (JAWRA)* 49(6): 1327- 1350.

Howell, T.A. (2001). Enhancing Water Use Efficiency in Irrigated Agriculture. *Agronomy Journal*, *93*(2), 281–289. https://doi.org/10.2134/agronj2001.932281x

Huntington, J., Gangopadhyay, S., Spears, M., Allen, R., King, D., Morton, C., Harrison, A., McEvoy, D., & Joros, Andrew. (2015). West-Wide Climate Risk Assessments: Irrigation Demand and Reservoir Evaporation Projections. 10.13140/RG.2.1.1209.8647.

Idaho Department of Water Resources (2013). *Enhanced Snake Plain Aquifer Model Version 2.1* [Final Report].

Irmak, S., Odhiambo, L. O., Kranz, W. L., & Eisenhauer, D. E. (2011). *Irrigation Efficiency and Uniformity, and Crop Water Use Efficiency*. 9.

Kale, R. V., & Sahoo, B. (2011). Green-Ampt Infiltration Models for Varied Field Conditions: A Revisit. *Water Resources Management*, *25*, 3505–3536.

Lamm, F. R., & Porter, D. O. (2017). Ogallala aquifer program center pivot irrigation technology transfer effort. Proc. Irrigation Association Tech. Conf. Fairfax, VA: Irrigation Association. Retrieved from https://www.ksre.k-state.edu/irrigate/cptt/Lamm_IA_17CPTT_FD.pdf

Leib, B., & Grant, T. (2019). *Understanding Center Pivot Application Rate*. 3.

Liang, X., Neibling, H., Yang, R. (2019). Evaluating LESA Irrigation Systems in Potato Production in Southern and Eastern Idaho. *BUL 933*. University of Idaho. https://www.extension.uidaho.edu/publishing/html/BUL933-Evaluating-LESA-Irrigation-Systems-in-Potato-Production.aspx.

Liu, Y., Pereira, L.S., & Fernando, R.M. (2006). Fluxes through the bottom boundary of the root zone in silty soils: Parametric approaches to estimate groundwater contribution and percolation. *Agricultural Water Management*, *84*(1–2), 27–40. https://doi.org/10.1016~ /j.agwat.2006.01.018

Miller, K., Goulden, P., Milman, A., & Tracy, M.K.J. (2019). Eastern Snake Plain Aquifer Recharge Project. 13.

Morari, F., Harb Rabia, A., Lo Presti, S., Gobbo, S., & Vellidis, G. (2020). Remote Sensing of Evapotranspiration Using SEBAL and Metric Energy Balance Models for Enhanced Precision Agriculture Cotton Irrigation Scheduling. *EGU General Assembly Conference Abstracts*, 22272.

Morton, C.G., Huntington, J.L., Pohll, G.M., Allen, R.G., McGwire, K.C., & Bassett, S.D. (2013). Assessing Calibration Uncertainty and Automation for Estimating Evapotranspiration from Agricultural Areas Using METRIC. *JAWRA Journal of the American Water Resources Association*, *49*(3), 549–562. https://doi.org/10.1111/jawr.12054

Ogata, G., & Richards, L.A. (1957). Water Content Changes Following Irrigation of Bare-Field Soil That is Protected from Evaporation. *Soil Science Society of America Journal*, *21*(4), 355–356. https://doi.org/10.2136/sssaj1957.03615995002100040001

Olson, R., Budge, R., & Budge, T.J. (2016). Summary of ESPA Settlement Agreement. *Idaho Law Blog*. https://www.racinelaw.net/blog/summary-espa-settlement-agreement/

Owen, Dave. (2014). Overallocation, Conflict, and Water Transfers. 9 Envtl. Res. Letters. Available at: https://repository.uchastings.edu/faculty_scholarship/1245

Patton, B. (2011). *Eastern Snake Plain Managed Aquifer Recharge Program*. Henrys Fork Basin Study Working Group.

Perry, C.J, & Steduto, P. (2017). *DOES IMPROVED IRRIGATION TECHNOLOGY SAVE WATER? A review of the evidence*. https://doi.org/10.13140/RG.2.2.35540.81280

Peters, R.T., Hoogenboom, G., & Hill, S. (2019). *Simplified Irrigation Scheduling on a Smart Phone or Web Browser*. 34.

Peters, T., Neibling, H., Stroh, R., Molaei, B., & Mehanna, H. (2019). *Low Energy Precision Application (LEPA) and Low Elevation Spray Application (LESA) Trials in the Pacific Northwest*. 23.

Richards, L.A., Gardner, W.R., & Ogata, G. (1956). Physical Processes Determining Water Loss from Soil. *Soil Science Society of America Journal*, *20*(3), 310–314. https://doi.org ~/10.2136/sssaj1956.03615995002000030004x

Ross, E., & Hardy, L. (1997). Irrigation Guide. In *National Engineering Handbook* (p. 820). NRCS.

Running, K., Burnham, M., Wardropper, C., Ma, Z., Hawes, J., du Bray, M.V. (2019). Farmer adaptation to reduced groundwater availability. *Environ. Res. Lett.* 14 115010. https://iopscience.iop.org/article/10.1088/1748-9326/ab4ccc/meta

Santos, C., Lorite, I. J., Allen, R. G., & Tasumi, M. (2012). Aerodynamic Parameterization of the Satellite-Based Energy Balance (METRIC) Model for ET Estimation in Rainfed Olive Orchards of Andalusia, Spain. *Water Resources Management*, *26*(11), 3267–3283. https://doi.org/10.1007/s11269-012-0071-8

Saxton, K.E., & Rawls, W.J. (2006). Soil Water Characteristic Estimates by Texture and Organic Matter for Hydrologic Solutions. *Soil Science Society of America Journal, 70*(5), 1569-1578.

Siebert, S., Burke, J., Faures, J. M., Frenken, K., Hoogeveen, J., Döll, P., & Portmann, F. T. (2010). Groundwater use for irrigation – a global inventory. *Hydrology and Earth System Sciences*, *14*(10), 1863–1880. https://doi.org/10.5194/hess-14-1863-2010

Šimůnek, J. (2015). Estimating groundwater recharge using HYDRUS-1D. *Geological Institute, Bulgarian Academy of Sciences*, *29*, 25–36.

Sukow, J. (2021). *Eastern Snake Plain Aquifer Model Version 2.2* (p. 190) [Model Calibration Report]. Idaho Department of Water Resources.

Steduto, P., Hsiao, T. C., Fereres, E., & Raes, D. (2012). *Crop yield response to water*. Food and Agriculture Organization of the United Nations. https://www.fao.org/3/i2800e/i2800e00.htm, *Accessed October 25, 2021*.

Sterling, R., & Neibling, W.H. (1994). *Final Report of the Water Conservation Task Force*. IDWR Report. Idaho Department of Water Resources, Boise.

Stewart-Maddox, N., Thomas, P., Parham, W. (2018). Restoring a world class aquifer: a brief history behind managed recharge & conjunctive management. The Water Report. July 2018; 173:1–9.

Stockle, C. O. and R. L. Nelson. (1996). Cropsyst User's manual (Version 2.0). Biological Systems Engineering Dept., Washington State University, Pullman, WA, USA.

Stubbs, M. (2016). *Irrigation in U.S. Agriculture: On-Farm Technologies and Best Management Practices*; Congressional Research Service Report, R44158; Congressional Research Service: Washington, DC, USA.

Tasumi, M., Allen, R., & Trezza, R. (2006). *Calibrating Satellite-Based Vegetation Indices to Estimate Evapotranspiration and Crop Coefficients*.

The Mathworks Inc. (2020). MATLAB. *Version 8.9.0 (R2020a)*. Natick, Massachusetts.

Trenberth, K. E., Fasullo, J. T., & Balmaseda, M. A. (2014). Earth's Energy Imbalance. *Journal of Climate*, *27*(9), 3129–3144. https://doi.org/10.1175/JCLI-D-13-00294.1

Tuthill, D.R., Rassier, P.J., & Anderson, H.N. (2013). *Conjunctive Management in Idaho* (No. 108; The Water Report, pp. 1–11). Idaho Water Engineering, LLC.

USDA. (2008). *Soil Quality Indicators* (p. 2). USDA Natural Resources Conservation Service. https://www.nrcs.usda.gov/Internet/FSE_DOCUMENTS/nrcs142p2_ -053288-pdf

Vaccaro, J. J. (2007). *A deep percolation model for estimating ground-water recharge: Documentation of models for the modular modeling system of the U.S. Geological survey* (Scientific Investigations Report No. 2006–5318; p. 30). U.S. Geological Survey.

Vano, J.A., Scott, M.J., Voisin, N., Stöckle, C.O., Hamlet, A.F., Mickelson, K.E.B., Elsner, M.M., & Lettenmaier, D.P. (2010). Climate change impacts on water management and irrigated agriculture in the Yakima River Basin, Washington, USA. Climatic Change, 102(1–2), 287–317. https://doi.org/10.1007/s10584-010-9856-z

Wang, Z., Feyen, J., van Genuchten, M.T., & Nielsen, D.R. (1998). Air entrapment effects on infiltration rate and flow instability. *Water Resources Research*, *34*(2), 213–222. https://doi.org/10.1029/97WR02804

Ward, F. A., & Pulido-Velazquez, M. (2008). Water conservation in irrigation can increase water use. *Proceedings of the National Academy of Sciences*, *105*(47), 18215. https://doi.org/10.1073/pnas.0805554105

Ward, A.D., Trimble, S.W., Burckhard, S.R., & Lyon, J.G. (2016). *Environmental hydrology* (Third edition). CRC Press, Taylor & Francis Group.

Wilcox, J.C. (1959). Rate of soil drainage following an irrigation: I. Nature of soil drainage curves. *Canadian Journal of Soil Science*, *39*(2), 107–119. https://doi.org/10.4141/cjss59-015

Willardson, L.S., Allen, R.G., & Frederiksen, H.D. (1994). *Elimination of Irrigation Efficiencies*. 18.

WWAP (World Water Assessment Programme). (2012). *The United Nations World Water Development Report 4: Managing Water under Uncertainty and Risk.* Paris, UNESCO.